REE fractionation during granite weathering and removal by waters and suspended loads: Sr and Nd isotopic evidence

Dominique Aubert, Peter Stille, Anne Probst

REE fractionation during granite weathering and removal by waters and suspended loads: Sr and Nd isotopic evidence

DOMINIQUE AUBERT, PETER STILLE,* and ANNE PROBST†

ULP-Ecole et Observatoire des Sciences de la Terre-CNRS, Centre de Géochimie de la Surface, UMR 7517, 1 rue Blessig, 67084 Strasbourg, France

Abstract—Very few studies deal with REE (rare earth element) mobility within the system soil–soil solution–streamwater. In this article, we try to characterize the fractionation and the migration of the REE in a granite-derived soil system located in a small catchment of the Vosges mountains. ICP-MS and TIMS measurements were performed on both solid samples ("fresh" granite, soil, and suspended load of the stream) and waters (soil solutions, springwater, and streamwater) to determine their respective REE concentrations and Sr and Nd isotopic compositions. The PAAS-normalized REE pattern of the bedrock is characterized by a strong depletion in HREE (heavy REE) and a negative Eu anomaly (0.46). Similarly, the granite-normalized REE distribution patterns of the soil samples show HREE depletions that become more important with decreasing depth. The correlative behavior between P_2O_5, Th, and REE with depth indicates that, besides apatite, other phosphate minerals such as monazite are the most important phases controlling the Th and REE budget in the soil profile. On the other hand, at greater depth, zircon seems to be another important mineral phase controlling especially the HREE enrichment as shown by the positive relationship between Zr content and the Yb/Ho ratio. Different grain size fractions show similar REE distribution patterns and are only weakly fractionated, compared with bulk soil sample. However, the finest fraction (0–20 μm) is more enriched in Sr and REE, suggesting a stronger concentration of REE-carrying minerals in this fraction. The suspended and dissolved load of the stream show as a whole an enrichment in HREE if compared with the granite or with the different soil samples. However, compared with the uppermost soil samples, the suspended load is significantly more enriched in HREE. Its REE distribution pattern is more similar to that of the finest fraction of the deeper soil sample and to the "fresh" granite. Thus, most probably the REE of the suspended load originated from a source with REE characteristics found in the deep soil horizons. This source might have been situated in the uppermost soil profile, which is actually REE depleted. The weathering process can be compared with a leaching experiment where the waters correspond to the leachate and the soil to the residual phase of the granite. The Sr isotope data indicate that the suspended load originates from the finest soil fraction. The Sr and Nd isotopic data of the suspended load suggest that it contains up to 3% Sr and Nd from apatite and up to 97% from feldspar. Most of the Sr and Nd in the waters originate from apatite leaching or dissolution.

1. INTRODUCTION

Chemical and mechanical weathering leads to the disaggregation of rocks and minerals and the formation of soil systems, and it allows the removal of chemical elements as well as of larger and smaller particles from altered rocks and soils by rain-, pore-, spring- and riverwater. Major river systems have been studied to estimate the fluxes of continent-derived material to the oceans, to determine erosion source parameters, to describe erosion processes, and finally to calculate denudation rates and global geochemical budgets (Martin and Meybeck, 1979; Stallard and Edmond, 1983; Meybeck, 1987; Négrel et al., 1993; Blum et al., 1994; Amiotte-Suchet and Probst, 1995; Drever and Clow, 1995; Gaillardet et al., 1995; Allègre et al., 1996; Dupré et al., 1996; Gaillardet et al., 1997).

The physicochemical processes leading to in situ production of the detrital soil components and the release and mobilization of REE during alteration are well-documented (Nesbitt, 1979; Braun et al., 1990; Nesbitt et al., 1990; Condie, 1991; Braun et al., 1993; Boulange and Colin, 1994; Condie et al., 1995; Koppi et al., 1996; Nesbitt and Markovics, 1997; Steinmann and Stille, 1997; Braun et al., 1998; Sharma and Rajamani, 2000). From all these studies it becomes evident that the REE mobility is mainly controlled by two factors, the climatic weathering conditions and the stability of the primary REE-carrying minerals.

Chemical weathering supplies the dissolved load to the rivers, whereas the rivers' suspended loads predominantly contain residual alteration products as well as secondary mineral phases that formed during weathering, such as clay minerals, oxyhydroxides, and phosphates. Secondary mineral phases and organic matter play an important role in the retention of the REE in the soil and may prevent REE from entering into circulating water systems (Stille et al., 1999). The importance of the replacement of primary REE-bearing minerals such as monazite, allanite, zircon, and apatite by secondary LREE-carrying phosphate minerals such as rhabdophane $(La,Ce,Nd)PO_4.nH_2O$, crandallite group $(REE)Al_3(PO_4)_2(OH)_6$, florencite $(La,Ce,Nd)Al_3(PO_4)_2(OH)_6$, Ce-Nd françoisite $(Ce,Nd)(UO_2)_3(PO_4)_2O(OH)6H_2O$ or uranium-bearing minerals such as coffinites (U-silicate) or uranyl-phosphate-

*Author to whom correspondence should be addressed (pstille@illite.u-strasbg.fr).

†*Present address:* Laboratoire des Mécanismes de Transferts en Géologie, UMR 5563, CNRS/Université Paul Sabatier, 38 rue des 36 Ponts, 31400 Toulouse, France.

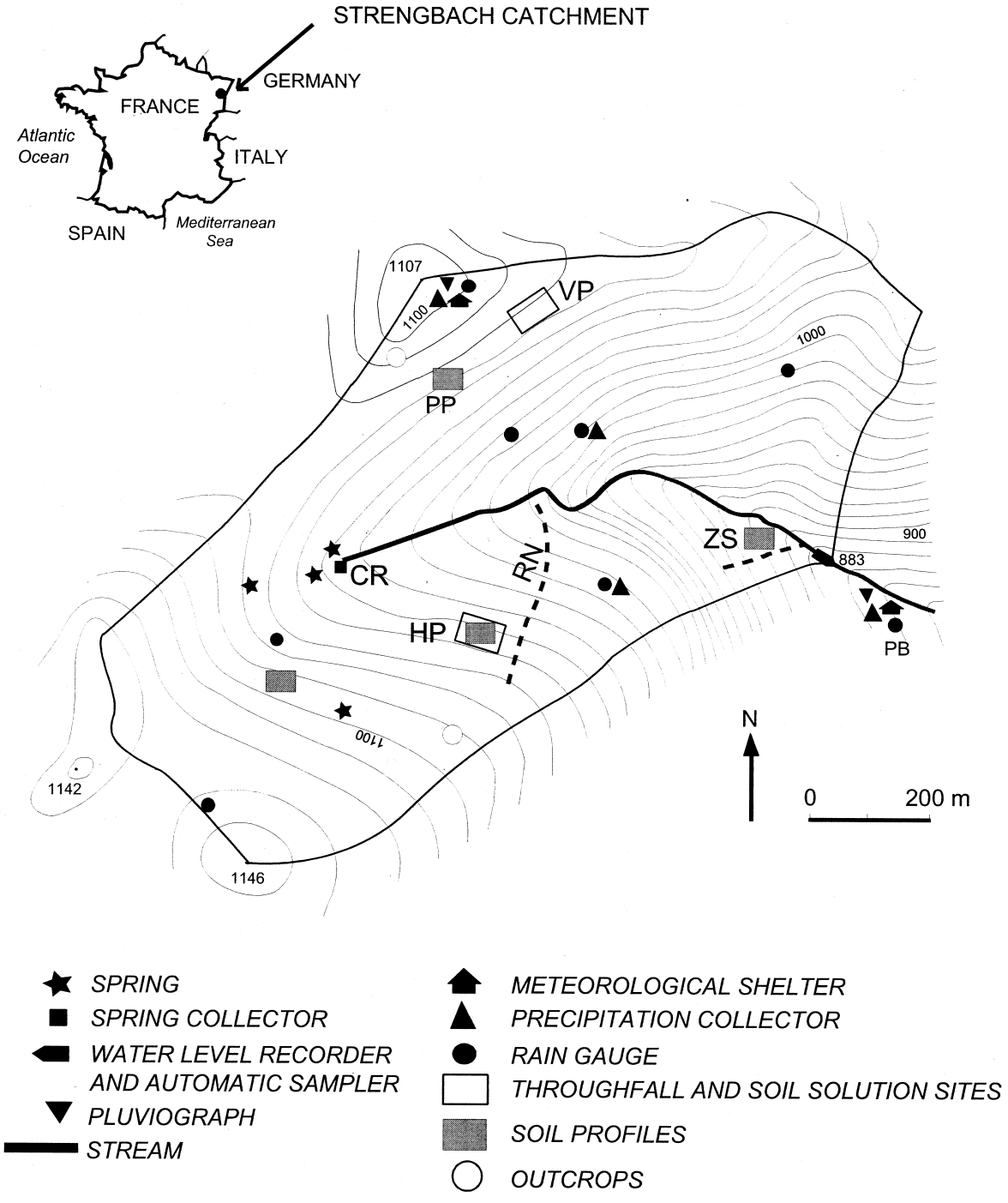

Fig. 1. Strengbach catchment with sampling sites.

hydrates was previously largely discussed (Banfield and Eggleton, 1989; Stille et al., 1999).

Several geochemical and isotopic studies have been performed on suspended particulate and dissolved river loads to provide information about their origin and to examine elemental fractionation between colloidal and solution phases for several major river systems (Goldstein et al., 1984; Stordal and Wasserburg, 1986; Goldstein and Jacobsen, 1987; 1988a; 1988b; Elderfield et al., 1990; Sholkovitz, 1992; Négrel et al., 1993; Douglas et al., 1995; Allègre et al., 1996; Henry et al., 1996; Tricca et al., 1999; Ingri et al., 2000). However, only a very few geochemical and isotopic studies that deal with REE mobility at the groundwater-soil interface (Banks et al., 1999; Stille et al., 2000) or that focus on the relationship between the REE characteristics of small streams, interstitial waters, and soils exist (Minarik et al., 1998). The only studies linking REE fractionation occurring in soil systems to those found in rivers or groundwaters have been performed on lateritic soil systems

Table 1. Mineralogical characteristics of the soils and the bedrock.

Samples	Depth (cm)	Quartz (%)	K-feldspar (%)	Plagioclase (%)	Clays + Micas (%)	Apatite (%)	Particle size
PP Soil[a]	0–20	38.6	10.9	5.4	45.9	0.05	<2 mm
	40–60	27.3	5.6	7.5	55.9	0.21	<2 mm
	60–80	27.8	7	8.7	53.5	0.42	<2 mm
	80–100	27.4	8.9	8.1	53.2	0.43	<2 mm
	100–120	27.2	12.8	10.6	46.6	0.43	<2 mm
	120–140	22.1	10.7	16.4	47.6	0.54	<2 mm
	140–160	21.9	7.2	17.8	50.8	0.42	<2 mm
	160–180	26.9	12.6	15.9	45.8	0.41	<2 mm
Bedrock[b]		36	18	33	9	0.5	—
ZS soil[c]	120	50	5.7	9.1	35	—	0–20 μm
		48	5.2	14.7	31.8	—	20–50 μm
		47	6	22.2	24.7	—	50–200 μm
		57	23	3.8	16.3	0.6	200–2000μm

[a] X-ray diffraction (data from Fichter, 1997) (% in weight).
[b] Counting on thin sections (data from Probst et al., 2000) (% in volume).
[c] X-ray diffraction (this study) (% in weight).

in humid tropical regions of East Cameroon and Gabon (Braun et al., 1998; Stille et al., 1999).

The aim of the present study is to elucidate the origin and the migration behavior of the REE in a soil system that formed at the top of a granite body within a small catchment of the Vosges mountains. It is of special interest to characterize the REE fractionation during weathering and migration processes in the soil and to determine their redistribution onto suspended load particulate phases and into "dissolved load" when reaching the streamwater at the outlet of the catchment.

2. GEOLOGICAL SETTING

The Strengbach forested catchment covering a 80-ha area is located on the eastern part of the Vosges Mountains (North East of France), 58 km SW from Strasbourg (Fig. 1). The elevation ranges from 883 m at the outlet to 1146 m at the top. The slopes are rather steep. The climate is temperate oceanic mountainous, and west wind dominates. The monthly averages of daily mean temperatures range from −2°C to 14°C (Probst et al., 1990). Rainfall is well spread all over the year; nevertheless, the most important precipitations occur in spring, whereas they are quite rare in autumn. Snowfall season lasts 4 months per year from December to April. The hydrological balance indicates for the 1986 to 1995 period a rainfall amount of ≈1400 mm/yr. The mean annual stream discharge reaches 20 L/s (Probst et al., 1995a).

The bedrock is a base-poor leucogranite (Brézouard granite). Its Rb-Sr whole rock isochron age is 315 ± 7 Ma (Bonhomme, 1967). This coarse grained granite has been affected by postintrusive hydrothermal fluids. It only outcrops at two locations (Fig. 1). At the top edge of the catchment, a banded gneiss lies in contact with the granite. The soils are rather deep (80 cm average), sandy and stony and lay on a saprolite that can reach 10 m depth. These soils belong to a brown acidic to ochreous

Table 2. Mean chemical composition of the soils (in % weight of dried sample at 110°C).

Soil	PPA1	PPAB	PPB1	PPB2	PPBC	PPC	Bedrock (HPT)[a]
Depth (cm)	5	30	60	90	120	180	
pH (water)	4.4	4.1	4.3	4.6	4.6	4.9	—
% O.M.	21.7	2.2	2	1.1	1.3	0.6	—
SiO_2	47.6	69.1	69.7	67	65.1	70.1	73.8
Al_2O_3	8.7	15.6	16.8	18.6	18.2	17.6	14.1
MgO	0.29	0.46	0.49	0.52	0.57	0.52	0.24
CaO	0.14	0.05	0.04	0.04	0.11	0.28	0.37
Fe_2O_3	1.2	2.1	2.2	2.2	2.2	1.9	1.08
Na_2O	0.38	0.59	0.48	0.55	0.43	0.66	3.68
K_2O	3.27	5.47	5.24	5.59	5.69	5.27	5.05
P_2O_5	0.2	0.2	0.26	0.25	0.38	0.35	0.27
Zr (ppm)	18.8	19.9	80.3	80.1	77.8	76.1	84
Th (ppm)	7.9	7.81	9.5	10.8	11	13.3	12.6

[a] Probst et al., 2000.
O.M., Organic matter.

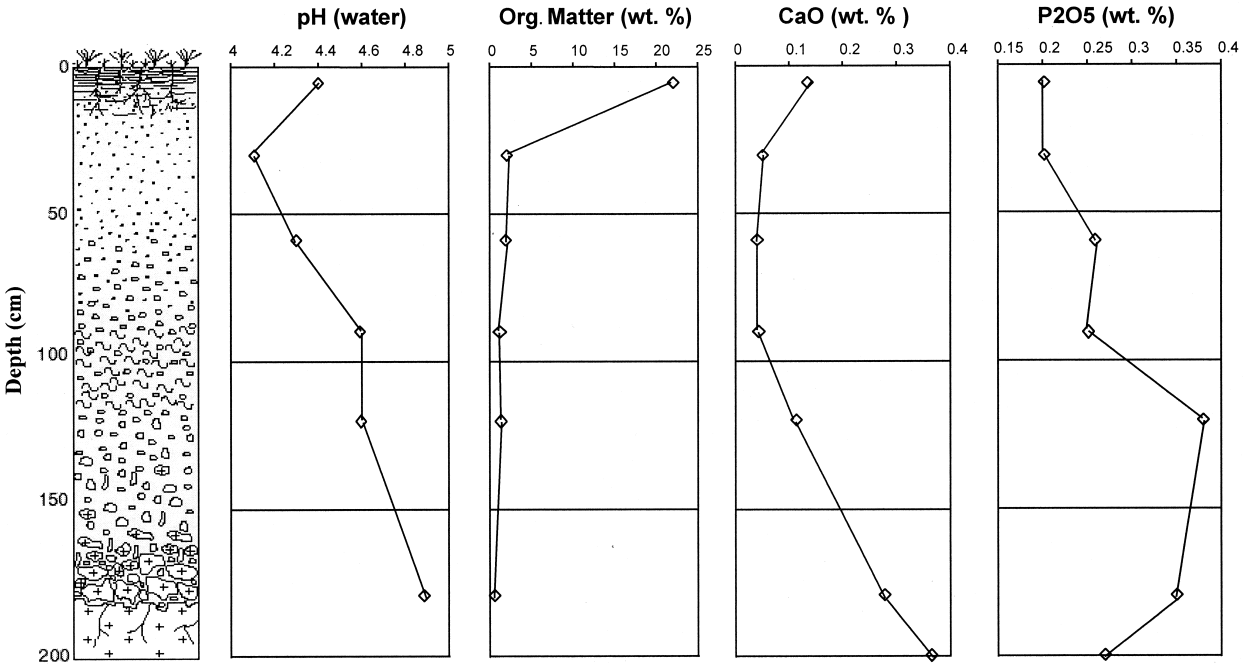

Fig. 2. Evolution of pH, organic matter, CaO and P_2O_5 within the soil profile.

podzolic soil series. A small hydromorphic zone, which only represents 2% of the total catchment area (Probst et al., 1990), takes up the valley bottom near the outlet. This area has been identified as a major contributor to streamwater during storm events (Idir et al., 1999). Weathering products and secondary mineral phases in soils and saprolite have been characterized (El Gh'Mari, 1995; Fichter et al., 1998). Hydrochemical budgets and denudation rates at the soil and catchment scale have been quantified (Dambrine et al., 1995; Probst et al., 1992; 1995a,b). Recently, Sr isotope ratios were used to trace the weathering processes (Probst et al., 2000). ($^{234}U/^{238}U$) activity ratios have been determined in streamwaters at the outlet to determine temporal variations of U disequilibrium (Riotte and Chabaux, 1999). Moreover, hydrological processes have been investigated for 15 yr in this catchment (Viville et al., 1993; Lu et al., 1995; Biron et al., 1997; Pfister et al., 1997; Ladouche et al., 2000).

3. SITE EQUIPMENT AND SAMPLING

The Strengbach catchment has been studied since 1986 and was originally monitored to observe the effects of acid rain on a forested ecosystem and more particularly on base cation availability (Probst et al., 1990; 1992). At four sites, bulk precipitation was regularly collected with PVC funnel collectors (during snow season, buckets are used). Throughfall is sampled by using 2-m-long open gutters, and soil solutions are collected at different depths by using zero-tension lysimeter plates.

Four springs rising 4 m down in the granite in the upper part of the basin are the main contributors to the stream. They flow into a general collector (CR), which is partly harnessed for drinking water supplies. Streamwater is controlled by a H-Flume notch weir, and water level is monitored both by ultrasonic and mechanical limnigraphs. Streamwater and springwater have been collected weekly. Three types of solutes have been selected for our study: spring water (CR), stream water (RS) sampled at the outlet, and interstitial waters (soil solutions) collected under the beech stand (SS) at 70 cm depth. Two different soil profiles have been sampled. The first one (PP) consists of a typic dystrochrept soil. The organic horizon is thin (only 10 cm) at the top of the profile (for more details, see Fichter et al., 1998). Deeper, the profile becomes more and more sandy. The saprolite is reached at 180 cm depth. The other soil profile called ZS is located in the hydromorphous area near the outlet. It is a dystric gleysoil with a rather thick O horizon (≈40 cm) composed of organic matter, roots, and

Table 3. REE concentrations (ppm) in granite and minerals.

	La	Ce	Pr	Nd	Sm	Eu	Gd	Tb	Dy	Ho	Er	Tm	Yb	Lu
HPT (granite)	16.3	37.51	4.66	17.28	4.14	0.35	3.09	0.49	2.45	0.37	0.82	0.12	0.69	0.09
Plagioclase	7.74	17.19	2.03	7.4	1.58	0.33	1.03	0.14	0.64	0.1	0.23	0.03	0.2	0.03
Orthoclase	3.97	8.94	1.01	3.71	0.83	0.48	0.59	0.08	0.33	0.05	0.11	0.01	0.09	0.01
Apatite	103.28	298.05	51.21	276.8	132.83	9.99	109.1	16.8	71.36	9.37	16.93	2.33	11.87	1.45
Muscovite	3.15	7.93	0.95	3.49	0.89	0.04	0.66	0.11	0.56	0.09	0.18	0.03	0.15	0.02
Biotite	60.72	147.08	17.73	66.22	14.05	0.24	9.8	1.36	5.9	0.86	1.86	0.26	1.37	0.19

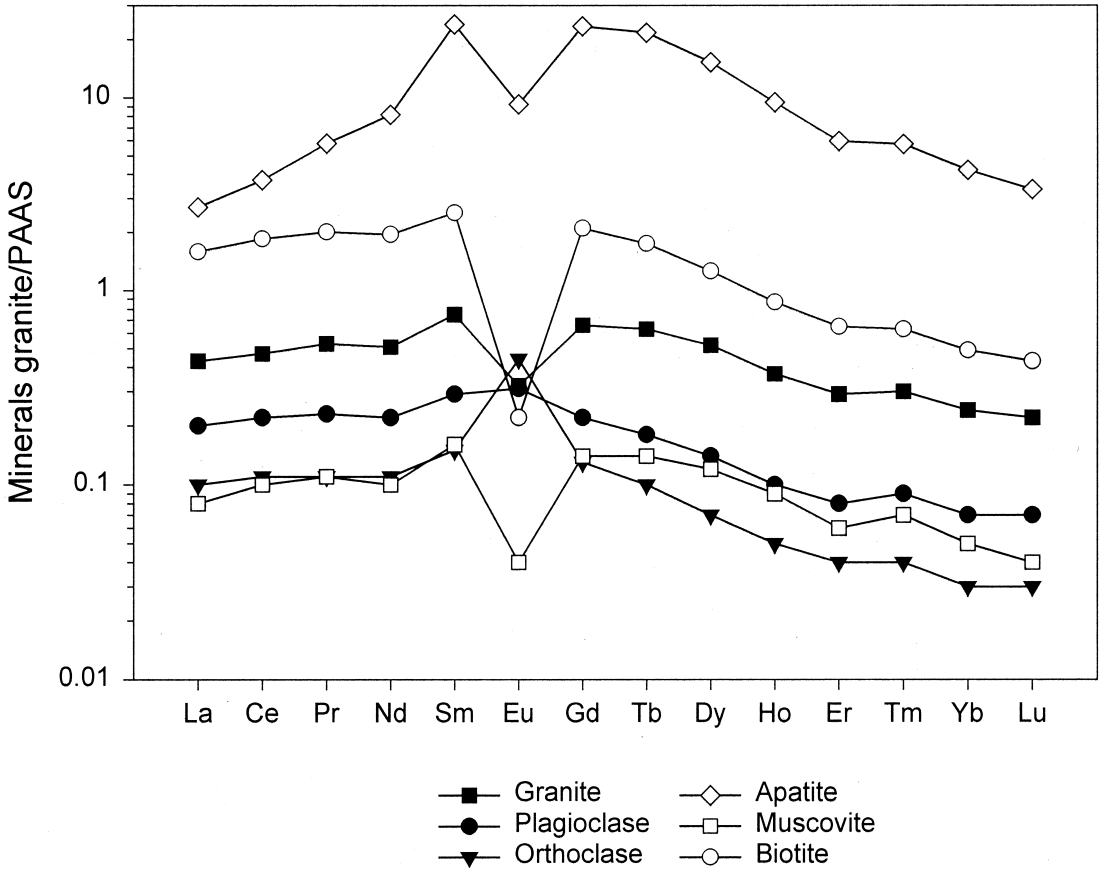

Fig. 3. PAAS-normalized REE patterns of the granite and the corresponding minerals.

quartz grains. At greater depth the soil becomes coarser. The fine earth (<2 mm) at 90 cm depth contains 6% clay and 73% coarse fraction (>0.2 mm). Deeper at 100 cm depth fine sand and gray clay layers have been found.

4. ANALYTICAL METHODS

The water samples were filtered on site through 0.45-μm pore size Millipore filters. The solution that passed this filter is called the dissolved load. It consists of dissolved ions and <0.45-μm colloids. The filtered samples were acidified with HCl to reach a pH between 1 and 2. A non acidified aliquot was kept to determine major elements, alkalinity, conductivity, and dissolved organic carbon (DOC). pH was measured on site by using a pH meter (Knick 651) with a combined electrode and in the laboratory by using the Mettler DL40GP memotitrator.

The REE were determined by inductively coupled plasma mass spectrometry (ICP-MS, VG PlasmaQuad PQ2+). The detection limit is 0.01 μg/L and the error of measurement < 5%. The REE concentrations of our water samples, however, are lower and, therefore, a specific enrichment method was required. A liquid–liquid extraction technique using HDEHP as organic solvent was applied to enrich the REE by a factor of at least 100 (Shabani et al., 1992; Tricca, 1997). Samples (0.5–2 L) were necessary to achieve concentrations above detection limit. The same extraction technique has been used to obtain sufficient

Table 4. REE concentrations (ppm) in the soil (<2 mm) and the soil grain size fractions.

PP soil	La	Ce	Pr	Nd	Sm	Eu	Gd	Tb	Dy	Ho	Er	Tm	Yb	Lu
PPA1 (5 cm)	17.63	38.27	4.35	15.4	2.72	0.25	1.54	0.18	0.76	0.13	0.31	0.05	0.27	0.04
PPAB (30 cm)	14.09	34.59	3.57	12.33	2.1	0.17	1.14	0.12	0.52	0.09	0.21	0.03	0.2	0.03
PPB1 (60 cm)	13.71	30.87	3.5	12.03	2.13	0.17	1.23	0.16	0.76	0.14	0.36	0.06	0.41	0.06
PPB2 (90 cm)	14.29	31.96	3.66	12.6	2.28	0.18	1.38	0.17	0.81	0.14	0.35	0.06	0.37	0.05
PPBC (120 cm)	13.99	31.22	3.59	12.69	2.38	0.19	1.52	0.2	0.98	0.16	0.38	0.06	0.38	0.06
PPC (180 cm)	14.64	34.2	3.91	14.64	3.13	0.31	2.37	0.36	1.64	0.26	0.55	0.09	0.47	0.06
Bedrock	16.3	37.51	4.66	17.28	4.14	0.35	3.09	0.49	2.45	0.37	0.82	0.12	0.69	0.09
Soil grain size fractions from 100 to 120 cm depth														
ZSC2 (0–20 μm)	53.56	120.93	13.83	50	8.93	0.91	6.11	0.83	4.14	0.75	1.98	0.33	2.05	0.3
ZSC2 (20–50 μm)	34.81	76.7	8.89	31.93	5.89	0.64	4.02	0.54	2.76	0.49	1.26	0.2	1.26	0.18
ZSC2 (50–200 μm)	22.15	49.09	5.76	20.72	3.96	0.38	2.81	0.39	1.82	0.3	0.69	0.11	0.62	0.08
ZSC2 (200–2000 μm)	11.25	24.9	3.0	10.74	2.18	0.23	1.48	0.21	1	0.15	0.37	0.06	0.32	0.05

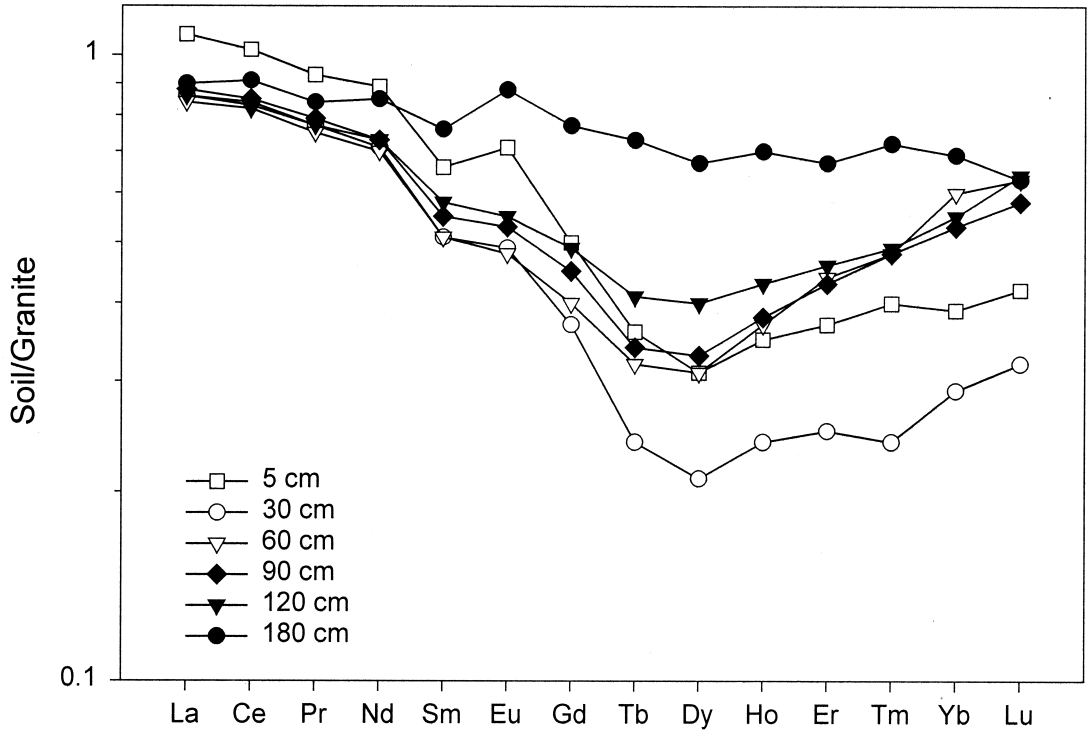

Fig. 4. REE distribution patterns of soils from different depths normalized to the fresh granite.

Nd (at least 20 ng) for isotope determinations using thermal ionization mass spectrometry. All Sr and Nd isotope analyses were performed on a fully automatic VG Sector mass spectrometer with a 5-cup multicollector after enrichment and separation of Sr and Nd from the bulk sample using cation-exchange resin.

The fresh bedrock minerals were separated from the 100- to 200-μm fraction of the granite by using magnetic separation (for muscovite and biotite), heavy liquids, and hand-picking techniques under optical binocular (quartz, plagioclase, and K-feldspar). Each mineral concentrate was finally checked by chemical analysis on scanning transmission electron microscope (STEM). The chemical composition of the granite and the soils was determined by using ICP-AES for major elements and ICP-MS for trace elements after digestion of samples in closed Teflon bombs containing a hot mixture (150°C) of HNO_3, HF, and $HClO_4$. We checked the efficiency of the triacid digestion method with the results achieved on PP soil profile and a BEN standard by using Li tetraborate fusion method. No significant difference in concentrations has been detected. The analytical precision is $<$10% for the ICP-AES and $<$5% for the ICP-MS on the first sigma level. The pH_{water} and the organic matter content of the soil have been determined at the Laboratoire d'Analyse des Sols (INRA, Arras) following classical methods (Baize, 1988).

The solid sample material (suspended load, bottom sediments, and soil samples) was considered to consist of two major phases: the unleachable detritus and the leachable pool (Sholkovitz et al., 1994). This is an operational definition because there is always a continuum between leachable and residual phases (Stille and Clauer, 1994; Steinmann and Stille, 1997). The REE from the leachable pool itself were considered to originate from two different reservoirs: the leachable detrital one and the labile reservoir, which includes all REE participating in solid–liquid interaction such as adsorption-desorption, surface complexation, coprecipitation, and leaching reactions. To separate the two major phases, we performed leaching experiments on the suspended load with 1 N HCl at room temperature for 15 min. To avoid readsorption (Sholkovitz, 1989) and to prevent buffering effects by dissolution of carbonate, the leaching experiments were performed by using a high acid/solid weight ratio of $\approx$1000. Leachates, residues, and corresponding untreated, total suspended loads were analyzed for REE and Nd isotopes. The unsoluble residual phases were digested for 7 days in closed Savilex vessels containing a hot mixture of HF, HNO_3, and $HClO_4$ acids. For Sr and bulk REE separation, 1-mL quartz columns with cation-exchange resin and ammonium citrate and HCl as eluents were used. Nd was separated from the remaining REE fraction by using the same type of columns and cation-exchange resin and α-hydroxyisobutyric acid as eluent.

For Sr and Nd isotope analysis, standard techniques were applied (Steinmann and Stille, 1997). Sr was loaded with nitric acid and Ta_2O_5 as activator on W single filaments. The ratio $^{86}Sr/^{88}Sr = 0.1194$ was used for fractionation correction. Typically, 100 ratios were collected to achieve adequate precision. During the measuring period, the NBS 987 Sr standard yielded $^{87}Sr/^{86}Sr = 0.710258 \pm 13$ ($\pm$sigma mean, $n = 9$). Nd was measured by using Ta-Re double filament assemblies. The ratio $^{146}Nd/^{144}Nd = 0.7219$ was used for fractionation correction. During the period of measurement the $^{143}Nd/^{144}Nd$ ratio of the La Jolla standard was 0.511856 ± 7 ($\pm$sigma mean, $n = 6$).

5. RESULTS AND DISCUSSION

5.1. Mineralogical and Major Element Compositions of the Soils

The mineralogical composition of the soil samples is shown in Table 1. Plagioclase is the most altered mineral of the soil. Its abundance is especially low at the surface (5.4%) but increases with depth. Its abundance at 120 to 180 cm depth, however, is still much lower ($<$18%) than that in the bedrock itself (up to 33%). Apatite is similarly depleted at the surface. K-feldspar, however, seems to be much less affected by weathering (Probst et al., 2000). X-ray diffraction performed on the ZS soil granulometric fractions from 120 cm depth indicates that K-feldspar is most abundant in the coarser fraction (200–2000 μm), whereas plagioclase mainly occurs in finer size fractions.

The chemical compositions of the soil samples and the bedrock are given in Table 2. The evolution of the organic

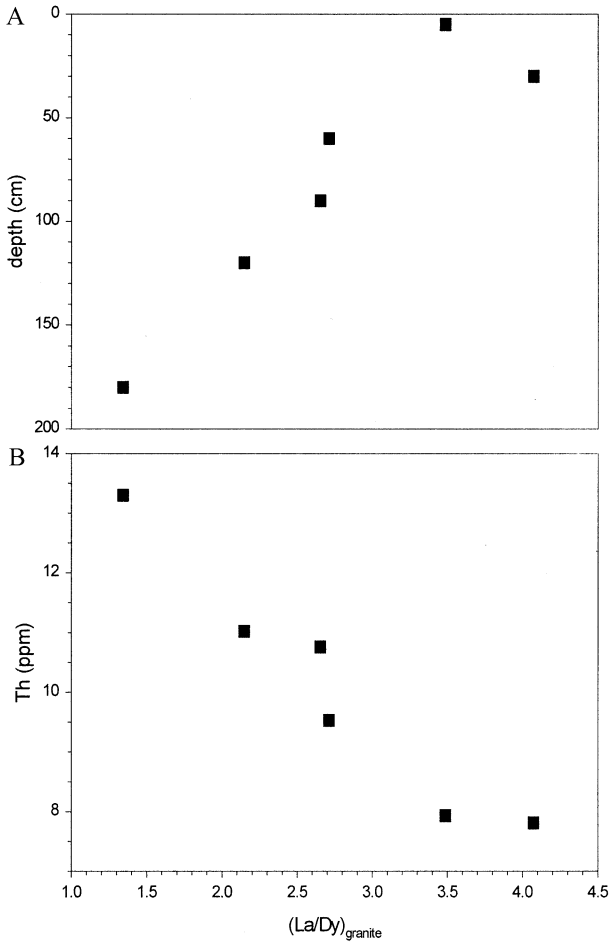

Fig. 5. (A) Depth-dependent correlation of HREE depletion expressed by granite-normalized La/Dy ratios of the different soil samples. (B) Correlation between lost of HREE and Th depletion.

matter, CaO– and P_2O_5– concentrations and pH of the soil with depth is shown in Figure 2. The surface horizon is enriched in organic matter (up to 20% wt.), whereas deepest horizons are depleted. The pH of the soil increases successively with depth from 4 to 5. A weak Ca enrichment can be observed for the uppermost soil sample probably due to atmospheric deposition (Probst et al., 2000) and/or smectites that are abundant in the shallower horizons of the soils. At greater depth (below 90 cm) CaO concentrations increase successively. The concentrations, however, remain below the bedrock value of 0.37% (wt.). Similarly, the P_2O_5 concentrations slightly increase with depth, indicating that apatite and other phosphate-bearing minerals are more abundant at greater depth of the soil profile.

5.2. The REE Data of the Fresh Granite

The REE concentration data of the "fresh" bedrock (HPT) and its minerals are compiled in Table 3. The PAAS-normalized REE pattern of the fresh granite is characterized by a strong negative Eu anomaly (Eu/Eu*) (McLennan, 1989) and a strong depletion in HREE (Fig. 3). The patterns strongly resemble that of monazite (McLennan, 1989 and cit. therein). However, the Eu anomaly (0.46) and the HREE depletion expressed by the PAAS-normalized (La/Yb)N of 1.7 are smaller than those of monazite with Eu/Eu* and (La/Yb)N of 0.16 and 15, respectively.

Muscovite and biotite have REE distribution patterns that are likewise similar to that of their host-rock (Fig. 3). The negative Eu anomaly of biotite, however, is stronger (0.1) than that of muscovite (0.25) or of the host-rock itself. It is comparable with that of monazite. The apatite also has a negative Eu/Eu* (0.39) but in contrast to its host-rock, it shows a hump-shaped REE pattern with HREE and LREE depletion. The Eu anomaly of plagioclase is positive but very small (1.22). Therefore, orthoclase is the only mineral in this granite carrying a strong positive Eu/Eu* of 3.23.

5.3. The REE Data of the Soil

The REE concentrations of the soil samples are compiled in Table 4. The granite-normalized REE distribution patterns of the soil samples show a HREE depletion that increases with diminishing depth (Fig. 4). Thus, the deepest soil sample is for the fresh granite nearly not fractionated and only slightly depleted. The most depleted HREE is Dy. The heavier REE (Ho to Lu) manifest a smaller depletion. Therefore, the HREE depletion is expressed by the granite-normalized La/Dy (Fig. 5A). This ratio is not only negatively correlated with depth but also with Th (Fig. 5B). The deepest soil sample has a La/Dy ratio and a Th concentration close to that of the fresh granite. It has the highest Th concentrations and shows the weakest HREE depletion. Similarly, P_2O_5 is positively correlated with Th and negatively with the La/Dy ratio (Fig. 6). The correlative behavior between P_2O_5, Th, and HREE depletion strongly suggests that these elements are controlled by phosphate minerals such as apatite and monazite and that their dissolution becomes an important process toward the surface, thus controlling the REE and Th mobilization and budget in the soil. The granite-normalized REE distribution patterns (Fig. 7) of both apatite and the most fractionated soil (30 cm depth) are complementary and suggest that removal of phosphate minerals has led to the observed HREE depletion of this soil. Removal of phosphates has been observed already earlier (Fichter et al., 1998; Probst et al., 2000). Compared with the granite, a slight HREE (Ho to Lu) enrichment has been observed (Fig. 4). This enrichment, expressed by the granite-normalized Yb/Ho ratio, is correlated with the Zr concentration of the soil at least at greater depths (Fig. 8). The two uppermost samples (5–30 cm depth) are very depleted in Zr (19 ppm, Table 2) and plot far off the trend. High (Yb/Ho)N are accompanied by higher Zr concentrations. This might indicate that some of the HREE enrichment might be controlled by a strongly HREE-enriched mineral phase like zircon.

The pH of the soil solutions is an important factor controlling the mobilization and finally depletion of the REE in the soil. The solubility of REE increases like for most metals with decreasing pH and, therefore, the pH of the soil solutions that increases with depth (Dambrine et al., 1998) might be a reason why the upper part of the soil profile with lower pH (Fig. 2) and low content of REE-rich minerals has slightly lower REE concentrations than the deeper part of the soil profile. Thus, it is observable that not only the REE but also the Th and P_2O_5 concentrations increase with increasing depth in the soil profile

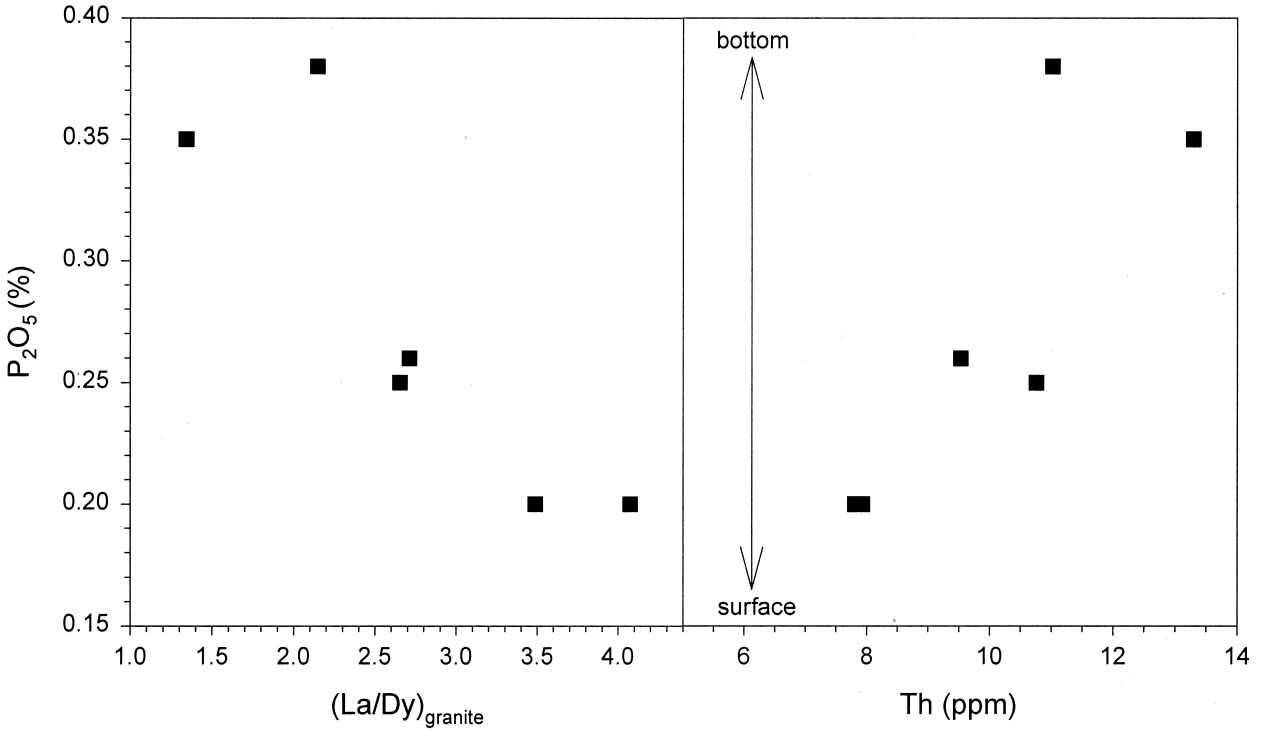

Fig. 6. Correlations between P_2O_5 contents, HREE, and Th depletion. Highest P_2O_5, Dy, and Th concentrations have been found at the deepest part of the soil profile close to the "fresh" bedrock.

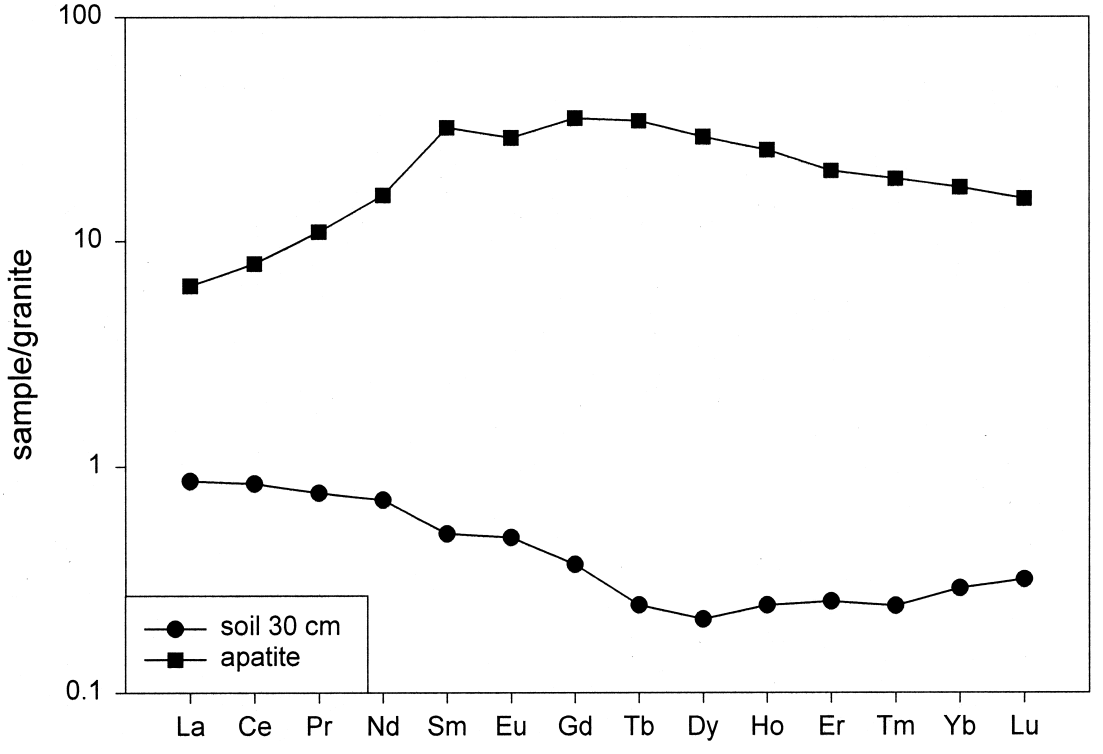

Fig. 7. Granite-normalized REE distribution patterns of apatite and the most REE-depleted soil sample from 30 cm depth.

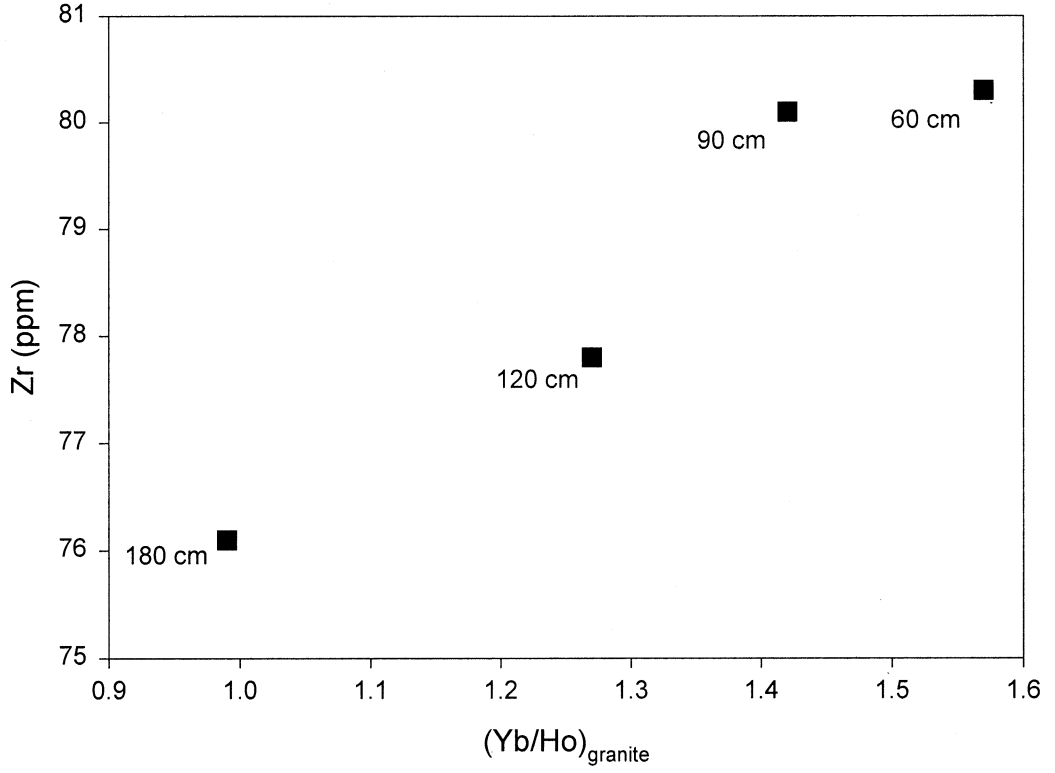

Fig. 8. Positive correlation between Zr and HREE enrichment expressed by the granite-normalized Yb/Ho ratio.

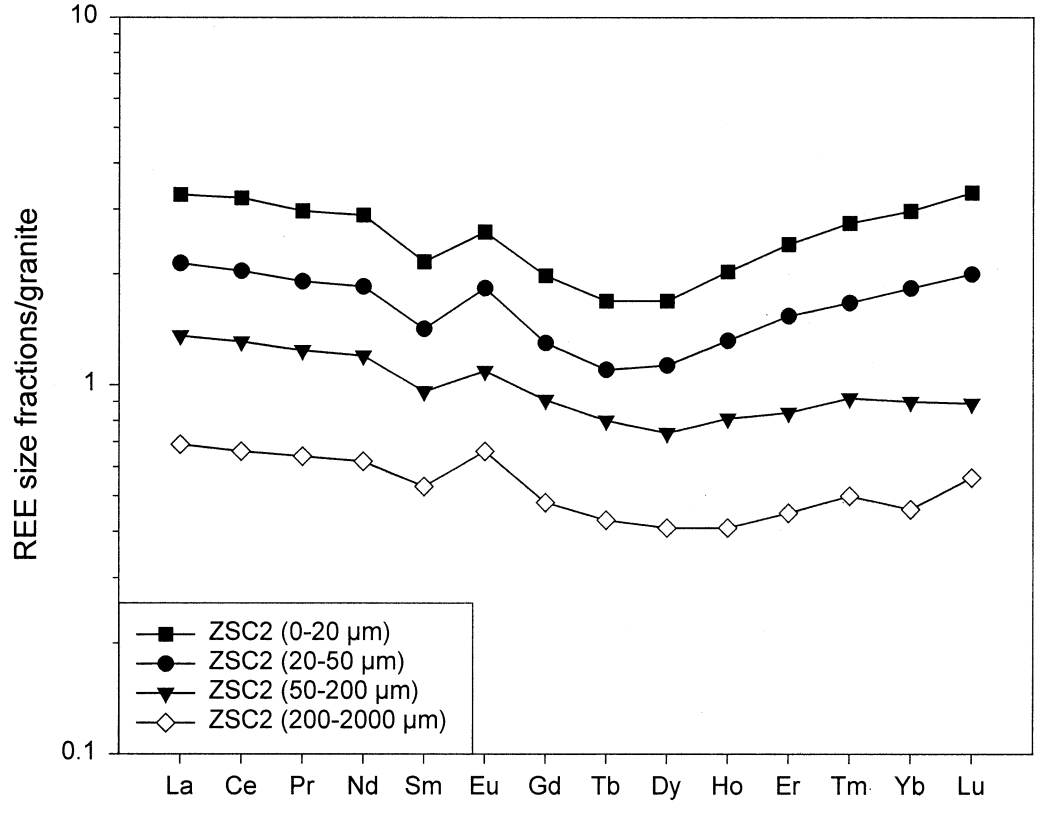

Fig. 9. Granite-normalized REE distribution patterns of different grain size fractions (<2000 μm) of the soil sample ZSC2.

Table 5. REE concentrations (ppm) of suspended loads.

Sample	La	Ce	Pr	Nd	Sm	Eu	Gd	Tb	Dy	Ho	Er	Tm	Yb	Lu
4108/33Leach	4.6	11.3	1.8	9	3.4	0.55	4.3	0.73	3.8	0.63	1.5	0.19	1.2	0.15
4109/23Leach	5.2	11.6	2.2	11.5	4.8	0.82	5.9	1	5.1	0.8	1.9	0.23	1.3	0.16
4112/35Leach	3.4	8.1	1.4	7.1	2.5	0.45	3.2	0.55	2.8	0.49	1.2	0.15	0.94	0.13
4108/33Susp	16.4	38.9	4.8	20.5	5.5	0.9	6.2	1	5.2	0.88	2.3	0.3	1.86	0.27
4109/32Susp	15.0	34.5	4.7	21.3	6.6	1.1	7.6	1.2	6.3	1.03	2.5	0.32	1.98	0.27
4112/35Susp	15.5	37.1	4.6	19.8	5.1	0.8	5.6	0.9	4.5	0.81	2.1	0.28	1.83	0.27
SS	23.7	9.3	0.99	3.67	0.93	0.18	0.95	0.2	1.08	0.17	0.41	0.07	0.36	0.05
CR	2.3	5.1	0.8	3.8	1.7	0.2	2	0.4	2.1	0.3	0.7	0.1	0.5	0.08

CR, spring water; SS, soil solution.
Streamwaters: 4108, 4109, and 4112 from Tricca et al. (1999).

(Figs. 5 and 6). The granite-normalized La/Dy, however, decreases with increasing depth. This suggests that during weathering processes the soil becomes more depleted in HREE and P_2O_5. Similar results have been found in a study on a soil profile at Bangombe (Gabon) (Stille et al., 1999). This finding can generally be explained by exchange of the soil with carbonate-rich waters that allow especially the HREE to form carbonate complexes (Johannesson et al., 1996; Steinmann and Stille, 1997). In the present case, however, the depletion cannot be explained by exchange of the soil with carbonate-rich waters because the catchment contains no carbonate. Nevertheless, Cantrell and Byrne (1987) have shown that solution complexation with organic ligands would produce the same HREE fractionation. Similarly, the complexation of Th with organic ligands can induce an increase of Th concentrations in natural waters with high dissolved organic carbon (DOC) contents (Langmuir and Herman, 1980; Munier-Lamy, 1987; Santchi and Honeyman, 1991; Viers et al., 1997). Because the soil solutions are rich in DOC (35 ppm as an average at 5 cm depth), a pH decrease toward the surface has probably contributed to the weathering-controlled dissolution of the phosphates, and solution complexation with organic ligands might have enhanced HREE and Th depletion in the solid phase.

None of the bulk soil samples collected at different depths of the soil profile has a positive Ce anomaly (Elderfield et al., 1990). Thus, no redox-controlled processes leading to CeO_2 precipitation seem to have occurred at the studied site, contrary to what was described earlier for lateritic soil profiles in humid tropical regions (Braun et al., 1993; Braun et al., 1998; Stille et al., 1999) and for heavy metal contaminated soils (Steinmann and Stille, 1997).

The four different grain size fractions (0–20 μm, 20–50 μm, 50–200 μm, and 200–2000 μm) from the ZS soil sample at 120 cm show identical REE distribution patterns (Fig. 9) that are also very similar to the bulk soil samples (PP) (Fig. 4). These patterns, therefore, suggest that the REE-carrying minerals are the same in all of these fractions and that not one of these minerals has been preferentially enriched in one of these fractions.

5.4. The REE Data of the Suspended and Dissolved Load

The REE concentration data of suspended and dissolved load are compiled in Tables 5 and 6, respectively. The suspended load is slightly enriched in HREE for granite and soil (Fig. 10). The La/Sm ratio normalized to the granite is close to 0.8 and expresses the LREE depletion. In addition, compared with the granite, the suspended load REE patterns show a strong positive Eu anomaly (1.46–1.63). Thus, on one hand, the soil is generally depleted in HREE for the granite (Fig. 4), and on the other hand, the suspended load is enriched in HREE. This reinforces the suggestion that especially the HREE but also Eu have been mobilized, removed from the soil, and finally deposited in the suspended load of the waters of the small stream in the Strengbach catchment. The suspended load is much more enriched in HREE than the soil sample from 30 cm depth as indicated by the low soil (30 cm) normalized (La/Yb)N ratio of 0.12. However, less HREE enriched is the suspended load compared with the soil sample from 180 cm depth, as suggested by the higher soil (180 cm) normalized (La/Yb)N of 0.27. This indicates that the uppermost part of the soil lost more REE and especially HREE than the deeper part of the soil. Nevertheless, this repartitioning of the HREE into residual soil and suspended particles cannot be due to a simple mechanical removal of fine-grained particles by surface waters. Indeed, similar Sr isotope data (Tables 7 and 8, Fig. 11) show that the suspended

Table 6. REE concentrations (ng/L) in the different surface waters.

	pH	La	Ce	Pr	Nd	Sm	Eu	Gd	Tb	Dy	Ho	Er	Tm	Yb	Lu
4108;33	—	21	34	7.2	41	17	3.1	20	3.8	22	4.1	12	—	13	2
4015;32	6.4	15	29	7	42	19	3.5	24	4.2	23	4.3	11	—	7.7	1.3
4109;32	6.2	16	39	8.8	56	23	4.1	29	5	27	4.6	12	—	11	1.6
SS	—	188.4	114.5	12.8	58	17.6	3.9	19.8	3.6	19	3.2	8.7	1.7	10.9	1.3
CR	5.9	50.5	174.2	33.2	195.2	95.3	16.6	151.5	26.5	145.3	23.4	57.2	7.3	49.5	7.1
RA	6.7	26.6	73.1	14.1	84.9	38.7	7	50	8.4	46.8	8.1	22.5	3.4	25.5	3.8

SS, soil solution; CR, spring water; RS, streamwater.
4015, 4108, 4109: streamwater (Tricca et al., 1999).

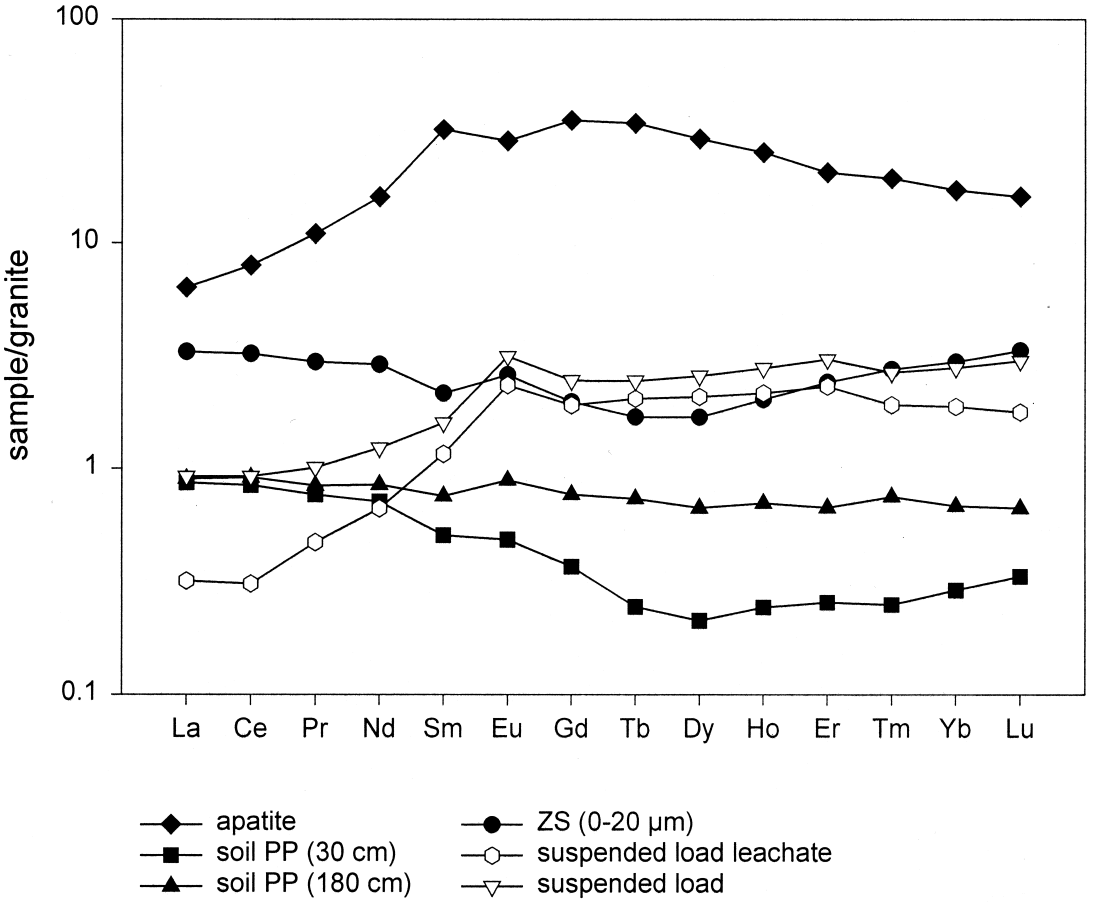

Fig. 10. Synthetic diagram showing granite-normalized REE distribution patterns of the most representative solid samples (apatite, soil samples from 30 to 180 cm depth, finest soil fraction and suspended load) and suspended load leachate.

particles represent the finest fraction of the original soil. But at the same time the REE patterns of the suspensions are clearly different from those of the finest soil fraction (<20 μm) at 100 to 120 cm. Thus, it is necessary to evoke a fractionation process that modified the original REE pattern of the fine soil particles during their transfer into suspension. A possible mechanism might be adsorption and/or coprecipitation of REE from soil solution onto the fine-grained particles when they were washed

Table 7. Nd isotope data of bedrock, apatite, soil samples, water samples and suspended load.

Solid samples	[Sr] ppm	[Nd] ppm	[Sm] ppm	Sm/Nd	$^{87}Sr/^{86}Sr$	$^{143}Nd/^{144}Nd$	εNd
Granite	42	17	4	0.24	0.838386(10)	0.512111(20)	−10.3
Apatite	790	276.8	132.8	0.48	0.716117(11)	0.512277(14)	−7
Soil 180 cm	44	14.6	3.13	0.21	0.816873(6)	0.512093(6)	−10.58
Soil 0–20 μm	106	49.1	8.9	0.18	0.753087(10)	0.512050(9)	−11.59
Soil 20–50 μm	82	31.9	5.9	0.18	0.765113(17)	0.512067(5)	−11.2
Soil 50–200 μm	52	20.7	4	0.19	0.811137(11)	0.512076(5)	−11
Soil 200–2000 μm	42	11	2	0.18	0.820177(10)	0.512088(6)	−10.9
Suspension 1	—	16.6	6.5	0.39	0.742642(10)	—	—
Suspension 2 total	—	20.5	5.5	0.27	0.741751(8)	0.512164(8)	−9.2
Suspension 2 residue	36.8	11.5	2.1	0.18	0.745444(8)	0.512102(8)	−10.5
Suspension 2 leach	21.7	9	3.4	0.38	0.720225(5)	0.512244(8)	−7.7
Water samples	**[Sr] μg/l**	**[Nd] ng/l**	**[Sm] ng/l**	**Sm/Nd**	$^{87}Sr/^{86}Sr$	$^{143}Nd/^{144}Nd$	εNd
Soil solution	7	58	17.6	0.30	0.722887(50)	—	—
Spring water	13	195.2	95.3	0.49	0.726062(23)	0.512242(38)	−7.66
Stream water	12	84.9	38.7	0.46	0.724811(29)	0.512237(11)	−7.81
Stream water 2	12	56	23	0.41	0.724473	0.512258(7)	−7.5

Suspension 2 and stream water 2 from Tricca et al., 1999.

Table 8. Sr isotope data of minerals and different grain size fractions of the soil at 120 cm depth.

Fract. ZS C2	Sample name	$^{87}Sr/^{86}Sr$	Sr (ppm)
Total	R4673	0.792631(9)	—
0–20 μm	R4882	0.753087(10)	—
20–50 μm	R4883	0.765113(17)	—
50–200 μm	R4884	0.811137(11)	—
200–2000 μm	R4885	0.820177(10)	—
>2 mm		0.805514(10)	
Minerals			
Granite		0.838386(10)	44.64
Muscovite		5.36858(6)	3.09
Biotite		5.86477(7)	4.3
Albite		0.774310(9)	73.67
Albite[a]		0.742029(5)	45.5
K-feldspar		0.797470(10)	77.02
Apatite		0.716117(11)	790.17

[a] From Probst et al. (2000).

out of the soil. Thus, the adsorbed or coprecipitated REE have a different origin and could stem from dissolution of REE-rich soil minerals such as apatite and/or monazite. This could also explain the similarity between the REE patterns of the leached suspended load and apatite (Fig. 10). Nevertheless, the suspended load mainly contains components of the smallest grain size fractions of the soil, as supported by the corresponding Sr isotope data. It is apparent from Figure 11 that the $^{87}Sr/^{86}Sr$ ratios vary as a function of grain size. The coarser grain size fractions (50–2000 μm) are the most radiogenic and show $^{87}Sr/^{86}Sr$ ranging between 0.820177 and 0.805514. The smaller grain size fractions are much less radiogenic with $^{87}Sr/^{86}Sr$ ranging between 0.753087 and 0.765113. The bulk sample has an intermediate Sr isotopic composition of 0.792631 as requested by mass balance. Therefore, the smaller the grain size the lower is the $^{87}Sr/^{86}Sr$. Moreover, the $^{87}Sr/^{86}Sr$ of the smallest soil fraction is close to that of the suspended load (0.745). The main secondary minerals in the clay fraction of the soils are regular interstratified illite-smectite (Probst et al., 2000). These clay minerals have a relatively high cation exchange capacity (CEC) compared with the coarser fraction and might therefore adsorb and carry an important part of not only Sr but also REE coming from dissolution of minerals or from atmospheric deposition.

The leachable reservoir of the suspended load shows an even stronger LREE depletion compared with the granite (Fig. 10). Its granite-normalized La/Sm ratio ranges between 0.27 and 0.35 and is similar to that of the dissolved load (0.2). Similarly, the Sm/Nd ratio of the suspended load leachate (0.38) is close to the ratios of the stream waters (0.41–0.46) (Table 7). This is supported by isotope data discussed in the next section.

The granite-normalized dissolved load REE distribution patterns of streamwater (Fig. 12A) are similar to those of the leachates of the corresponding suspended load (Fig. 10). It is

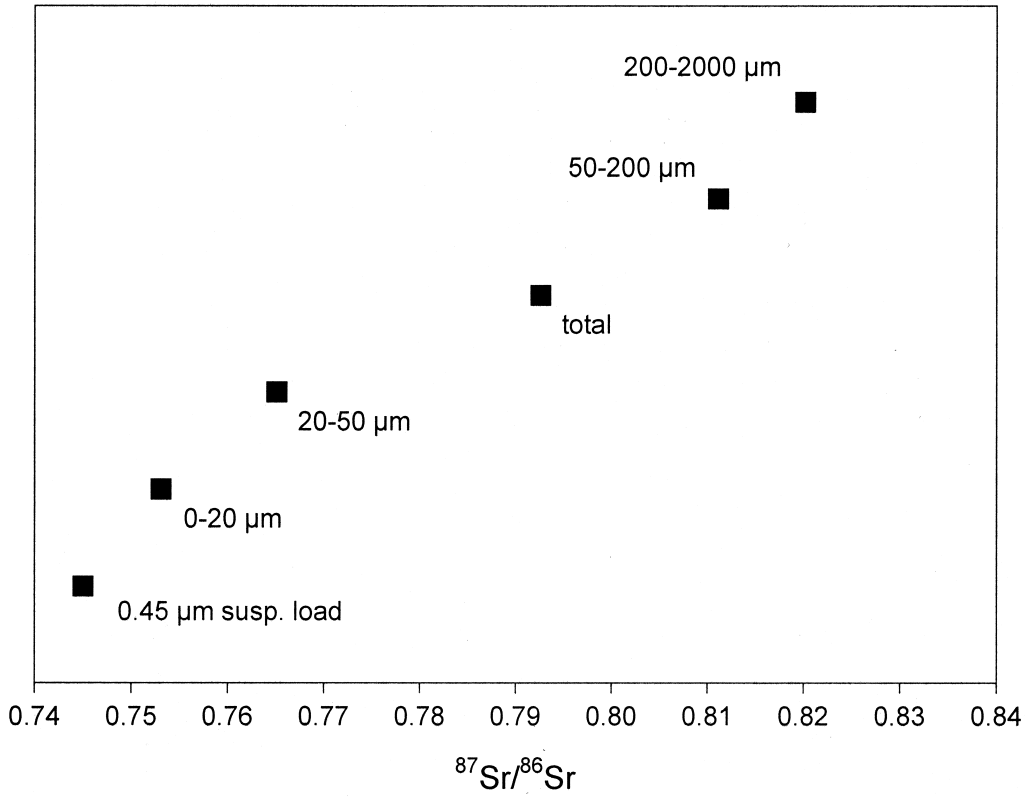

Fig. 11. Sr isotopic ratio of the suspended load compared with $^{87}Sr/^{86}Sr$ of different grain size fractions of the ZS soil from 120 cm depth.

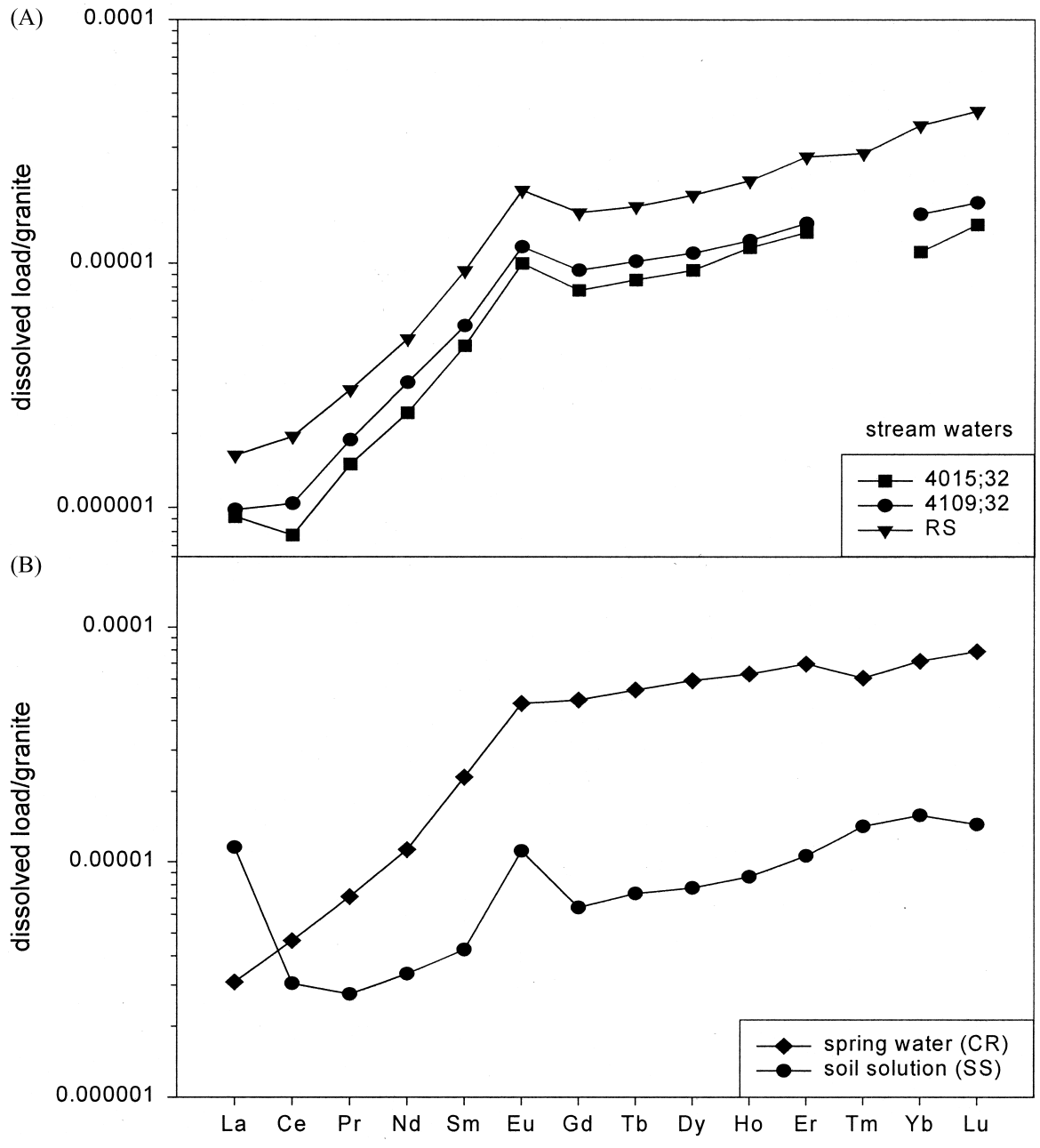

Fig. 12. Granite-normalized REE distribution patterns of dissolved loads. (A) Streamwater (RS, 4015 and 4109). (B) Soil solution SS and springwater CR.

even more LREE depleted than the corresponding suspended load. Similar to the suspended load or soil samples, soil solution (SS) and springwater (CR) show neither positive nor negative Ce anomalies (Fig. 12B). The REE patterns of the waters support, therefore, the suggestion that Cerianite precipitation is not an important mechanism in the studied soil profile. The pH of the soil solutions is rather low and ranges between 4 and 4.9. A negative Ce anomaly is much more frequent due to removal of Ce (IV) as CeO_2, which is the stable form of Ce in water at higher pH conditions (5–8) (Brookins, 1989; Tricca et al., 1999). This might explain why only the streamwaters with pH $>$ 6 show, compared with the granite, a very weak negative Ce anomaly (Fig. 12A).

For the granite, the streamwaters are likewise HREE and Eu enriched (Eu/Eu*: 1.8). This is also observed for soil solution (SS) and springwater (CR) (Fig. 12B). The soil solution shows a comparatively strong enrichment in La and Eu. These enrichments have been confirmed by repeated analysis and have also been found in the corresponding suspended load (Fig. 13). The Eu anomaly observed in the suspended and dissolved load suggests that weathering and corrosion of feldspar, especially orthoclase, is another important process controlling the release

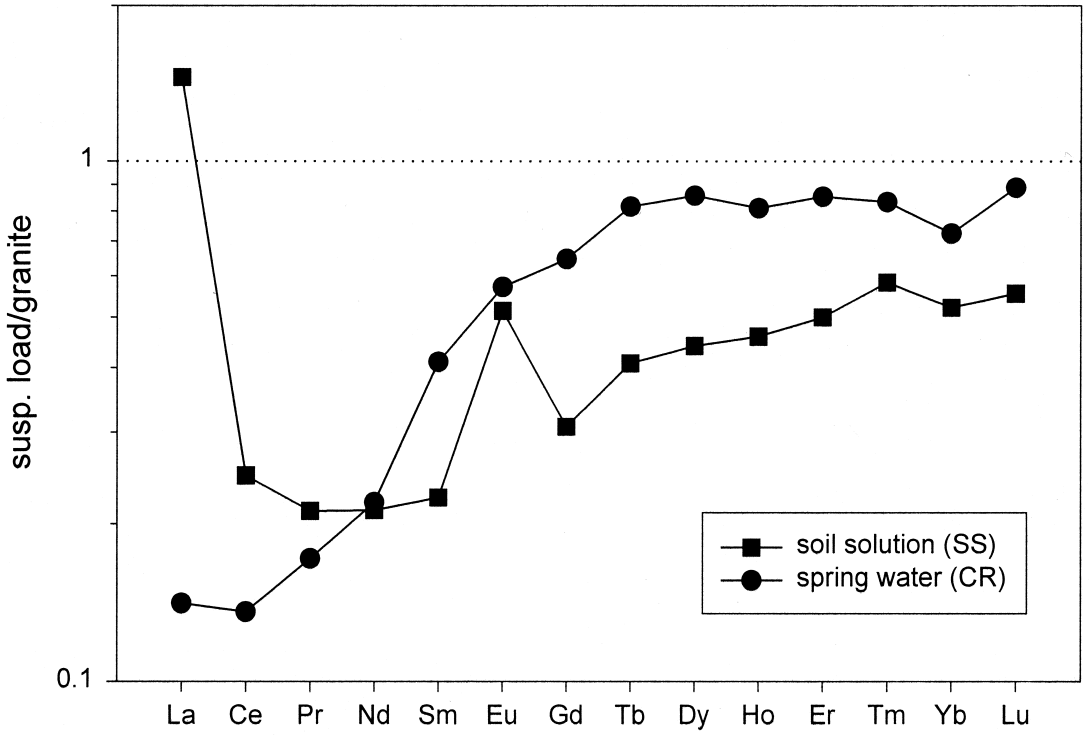

Fig. 13. Granite-normalized REE distribution patterns of suspended load from interstitial water (SS) and springwater (CR).

and mobilization of the REE and, therefore, their fractionation in the soil and their enrichment in the surrounding waters. This is confirmed by STEM observations and geochemical simulation of mineral weathering (Probst et al., 2000). The similarity between the REE distribution patterns of the dissolved (Fig. 12A) and those of the suspended loads (Fig. 10) suggests that the REE characteristics of small streams like the Strengbach are not yet significantly modified by the prevailing physicochemical conditions in the water. The dissolved REE in the streamwater seem to be in chemical equilibrium with the suspended load. Their distribution patterns are rather controlled by the principal lithologies in the corresponding drainage basins as already suggested earlier by Tricca et al. (1999).

Soil, suspended matter, and water samples have positive Eu anomalies compared with the granite, indicating that not all the phases derived from the granite weathering have been analyzed. The only other important components that might be complementary to soil, suspended load and waters and that have not yet been studied are the bottom sediments of the stream and the soil fraction $< 2\ \mu$m.

5.5. The Isotopic Relationships Between Bedrock Soil and Interstitial Streamwater

The Sr isotope ratios of the most important rock-forming minerals of the "fresh" and hydrothermally not strongly altered Brézouard granite (HPT) define a reference line in the Sr isochron diagram whose slope corresponds to an age of 311 Ma (not shown), which is in agreement with an earlier published Rb-Sr isochron age of 315 ± 7 Ma (Bonhomme, 1967). However, this age dates only approximately the intrusion of the granite because some of the data points plot off the reference line, indicating that even the so-called fresh granite has already been altered. Clay minerals that formed during hydrothermal overprinting and alteration yield K-Ar and Rb-Sr ages ranging between 150 and 180 Ma (El Gh'Mari, 1995).

The Sm-Nd isotope data of the granite, soil-saprolite (180 cm), soil fractions (0–20 μm and 200–2000 μm), and suspended and dissolved loads of the stream water define a "scatterchron" in an isochron diagram (Fig. 14), whose slope corresponds to an age of ≈200 Ma. This age is close to the hydrothermal event, but, nevertheless, from the statistical point of view it is geologically meaningless. The suspended load leachate shows like the water samples (stream and spring water) high Sm/Nd (>0.38) and $^{143}Nd/^{144}Nd$ ratios (0.51226), suggesting that their Nd and most probably also the other REE originate from the same source (Table 7; Fig. 14). The only mineral of the granite having that high Sm/Nd ratios and such a Nd isotopic ratio is apatite (0.48 and 0.51227, respectively; Tables 3 and 7). The corresponding suspended load residue, however, has similar to the soil samples low Sm/Nd (<0.21) and low $^{143}Nd/^{144}Nd$ (<0.5121). The untreated total suspended load plots as required from mass balance considerations between the values of corresponding leachates and residues. Because the catchment system consists primarily of one lithological unit and because atmospheric REE contribution is negligible, the basin can be considered as a more or less closed system with respect to Sm-Nd isotopes. Therefore, similar to the untreated total suspended load, the "fresh" granite plots between the isotopic

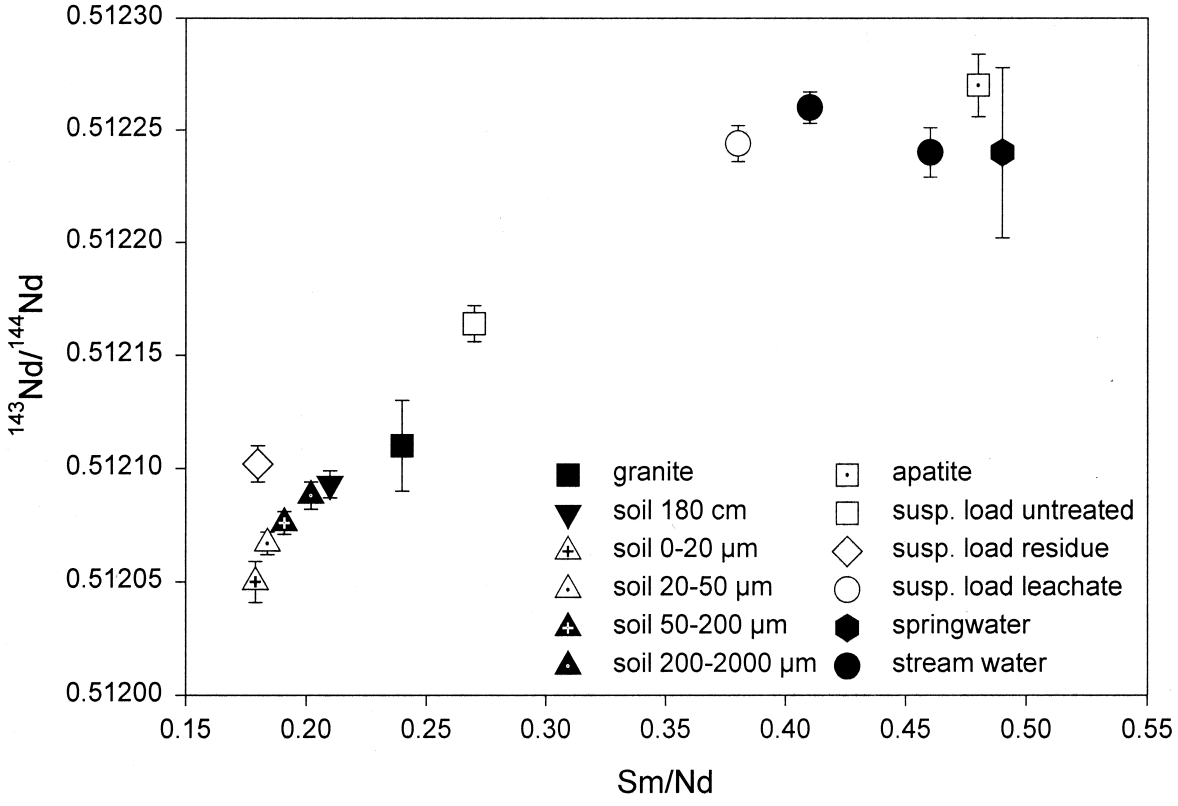

Fig. 14. Sm-Nd isotope data of streamwaters (RS, 4109) and corresponding suspended load and leachate, soil samples plotted in an isochron diagram.

composition values of the waters and the soil samples. Consequently, the weathering process is directly comparable with a leaching experiment where the waters correspond to the leachate and the soil to the residual phase of the granite.

The $^{87}Sr/^{86}Sr$ and $^{143}Nd/^{144}Nd$ isotope ratios are given in Figure 15. Two different alignments are recognizable, which have a common intersection (A) close to the small grain size fraction (0–20 μm). The other two end members are defined on the one hand by the surface waters (stream and springwater) and the suspended load leachate (C) with low $^{87}Sr/^{86}Sr$ and high $^{143}Nd/^{144}Nd$ of $\approx$0.720 and 0.51225, respectively, and on the other hand by relatively high $^{87}Sr/^{86}Sr$ of 0.838 and intermediate $^{143}Nd/^{144}Nd$ of 0.51211 for the whole rock (B).

The two alignments are controlled by the different mineral constituents of the granite. The $^{87}Sr/^{86}Sr$ and Sr concentrations are compiled in Table 8. The corresponding $^{143}Nd/^{144}Nd$ isotopic ratios have not been determined for all these minerals except for apatite, which has a Nd isotopic composition of 0.51227. This $^{143}Nd/^{144}Nd$ isotopic ratio combined with the measured Sr isotopic composition of 0.7161 yields point C in Figure 15. The other minerals $^{143}Nd/^{144}Nd$ isotopic ratios can approximately be deduced from their Sm/Nd ratios (Table 3) in Figure 14. The Sr isotopic composition of plagioclase and K-feldspar ranges between 0.742 and 0.797, respectively. Based on their Sm/Nd ratios (0.21, Table 3) a $^{143}Nd/^{144}Nd$ isotopic composition of 0.51205 can be deduced from Figure 14. Therefore, the intersection at A is defined by plagioclase. Consequently, the alignment AC suggests that the Nd and Sr of the suspended load mainly derive from feldspar, especially plagioclase, and apatite, whereas spring and streamwater would incorporate more Sr and Nd originating from apatite dissolution.

Two other major rock-forming minerals of the granite are biotite and muscovite. Their $^{87}Sr/^{86}Sr$ ratios are 5.8 and 5.4, respectively. Their Sm/Nd ratios (0.26 and 0.21, Table 3) allow to deduce a $^{143}Nd/^{144}Nd$ of $\approx$0.5121.

The Sr and Nd isotopic characteristics of the major mineral phases of the granite are shown in Figure 16A. The granite plots, as required from mass balance considerations, within the triangle defined by the isotopic characteristics of the different major rock-forming minerals. The diagram clearly shows the strong influence of plagioclase and apatite on the isotopic composition of the suspended and dissolved loads situated close to the line AC in Figures 15 and 16B. The Sr isotopic composition of point A in Figure 15 is close to that of the weathering end member (0.742) defined in this catchment by Probst et al. (2000). Otherwise, the diagram points to the rather weak influence of biotite and muscovite on the isotopic composition of the weathering products. This is in contrast to Blum and Erel (1997), suggesting that other easily weatherable minerals such as biotite contribute to a great extent to the Sr isotopic composition of streamwater.

Because Sr and Nd isotopic compositions as well as Sr and Nd concentrations of the plagioclase and apatite end members are well known, it is possible to calculate their contribution to

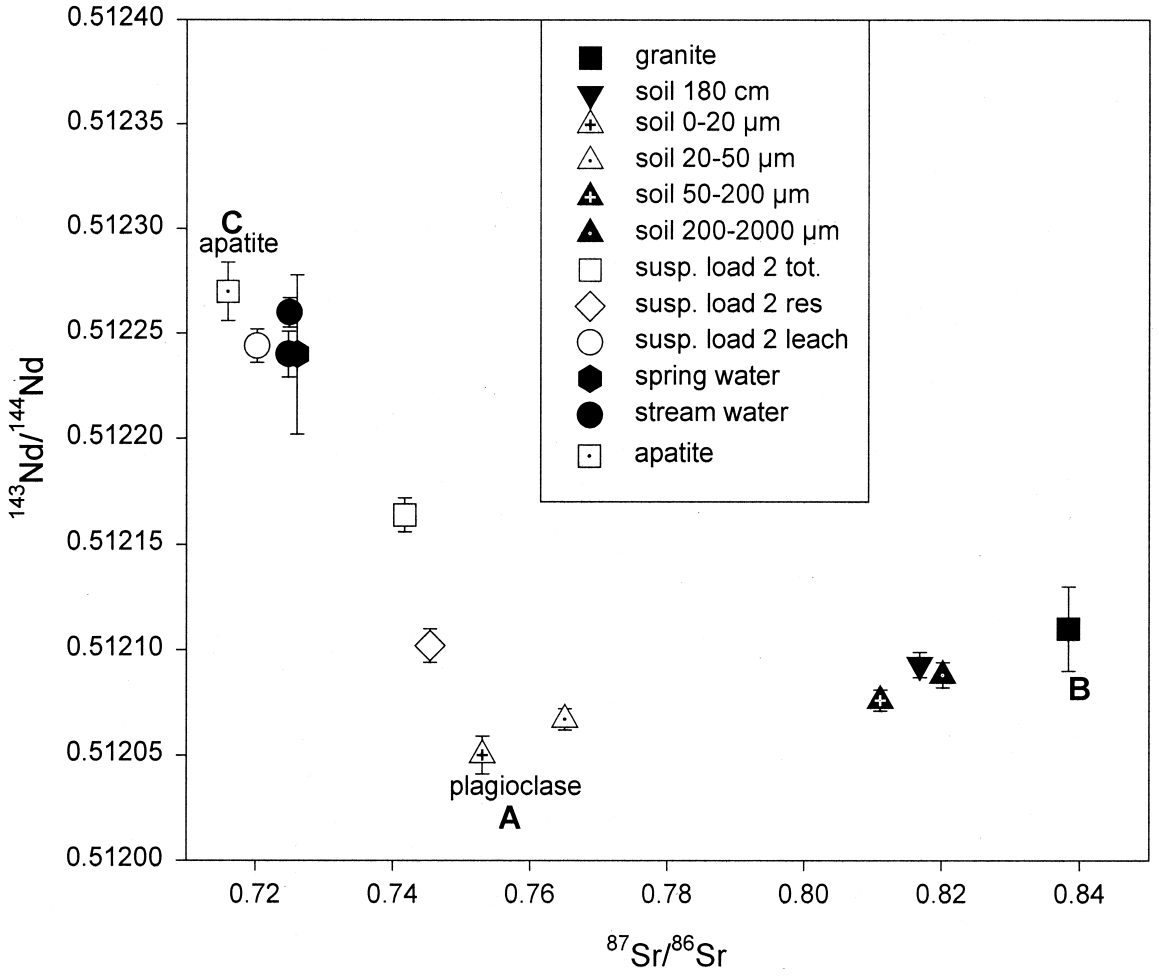

Fig. 15. Relationship between Sr and Nd isotopic compositions of solid and liquid phases.

the suspended load. The mixing curve is given in Figure 16B and marked off in terms of the weight fractions of apatite and plagioclase. The parameters used for mixing calculation are given in the figure caption. The mixing curve indicates that an even small apatite contribution of $<1\%$ changes significantly the Nd isotopic composition of the suspended load toward higher values. This is mainly due to the apatite Sr/Nd concentration ratio of ≈ 2.9, which is low compared with the much higher Sr/Nd ratio of 10 for the plagioclase. The mixing calculations suggest that the suspended load contains up to 3% Sr and Nd from apatite and up to 97% from feldspar, mainly plagioclase. However, the smallest soil fraction containing clay minerals with high CEC have Sr and Nd isotopic compositions that are closest to those of plagioclase or suspended load residue. Several authors suggest that these minerals might incorporate important quantities of Sr originating from atmospheric deposition (Graustein and Armstrong, 1983; Miller et al., 1993; Probst et al., 2000). Because no Nd isotopic composition data are available for this deposition, it remains difficult to discuss at this moment such a contribution based on the Sr-Nd isotope diagram of Figure 16.

6. SUMMARY AND CONCLUSIONS

The combined REE and Sr-Nd isotope study sheds new light into the weathering processes of a small silicate catchment and allows to trace the migration path of these elements as well as their removal by dissolved and suspended loads from small river systems.

The weathering of a granite leads to REE, especially HREE depletion. Within the soil profile the deeper parts are less depleted in HREE than the shallower parts. The pH evolution of the soil solutions with depth might be a reason why the uppermost part of the soil profile with lower pH is more depleted in REE than the lower part with higher pH. The correlative behavior between P_2O_5, Th, Zr, and REE with depth indicates that phosphate minerals such as apatite and monazite but also zircon are the most important phases controlling the Th and REE concentrations in the soil profile. Corrosion of feldspar especially orthoclase leads to Eu enrichments in suspended and dissolved loads.

The suspended and dissolved load of the stream shows as a whole an enrichment in HREE and, therefore, are the complementary parts of granite and soil. Compared with the uppermost

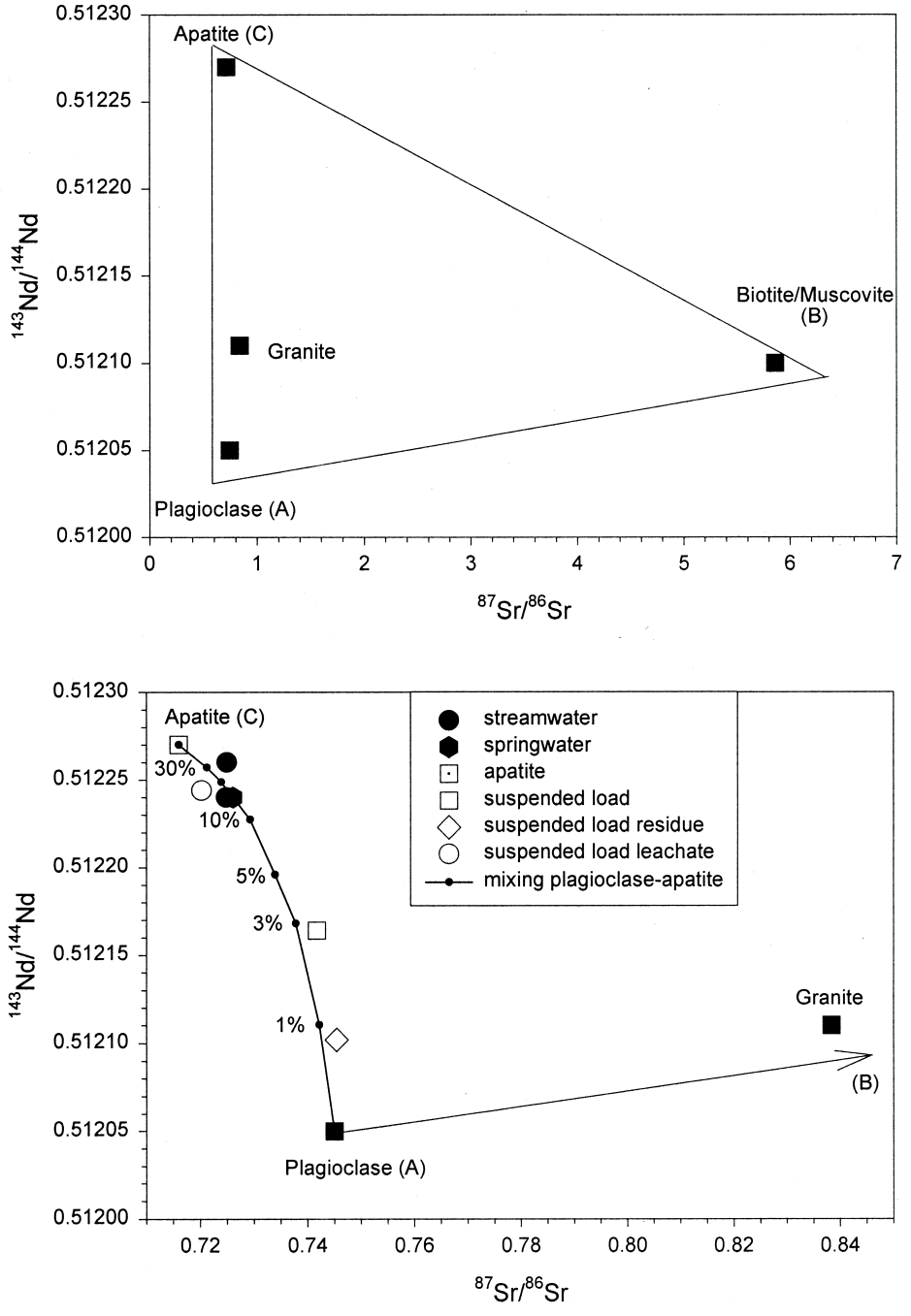

Fig. 16. Mixing model explaining Sr and Nd isotopic compositions of the granite (above) as well as of suspended and dissolved load (below). In the figure below the mixing curve is marked off in terms of the weight fraction of apatite and plagioclase. The following end member parameters have been used: apatite with $^{142}Nd/^{144}Nd = 0.51227$, $^{87}Sr/^{86}Sr = 0.716$ and Nd = 277 ppm, Sr = 790 ppm; plagioclase with $^{143}Nd/^{144}Nd = 0.51205$, $^{87}Sr/^{86}Sr = 0.745$ and Nd = 7.4 ppm, Sr = 73.7 ppm. The f-values indicate the percentage of apatite admixture to a plagioclase end member.

soil samples, the suspended load is significantly more enriched in HREE than the deepest soil sample or the "fresh" granite. Thus, most probably the REE of the suspended load originate from a source with REE characteristics found in the deep soil horizons close to the pristine granite within the weathering front. A similar source has also been situated in the uppermost part of the soil profile but actually leached out and depleted during recent weathering. One of the depleting processes can be related to the removal of the finest soil fraction (0–20 μm). The nearly identical Sr isotopic compositions of suspended load and finest soil fraction point to the close relationship between these two solid phases. The finest soil fraction is the most enriched in REE and Sr, suggesting a higher concentration of Sr and REE-carrying minerals in this fraction. Their removal, there-

fore, controls significantly the REE and Sr budget of the soil. Nevertheless, even this soil fraction is fractionated and slightly HREE depleted compared with the suspended or dissolved load. The Sm-Nd isotopic data suggest that this depletion can be related to a water–rock interaction that is comparable with a leaching experiment where the waters correspond to the leachate, which preferentially extracts the HREE and the soil to the residual HREE-depleted phase of the granite. This incongruent dissolution process has to be taken into account if global geochemical mass budgets and continental crust compositions are deduced from river-borne material (dissolved and particulate load; Gaillardet et al., 1995; Dupré et al., 1996). The Sm-Nd isotope relationship between water, suspended load, granite, and soil indicates that the average chemical composition of the altered granite can be deduced by summing the dissolved and the leached, residual soil.

The Sr and Nd isotope data allow one to approximately identify the principal components of the suspended load. Most important sources for Sr and REE are apatite, plagioclase, and to a lesser extent K-feldspar. Biotite and muscovite do not significantly contribute to the REE and Sr budget of the suspended load. Mixing calculations indicate that the suspended load contains up to 3% apatite and up to 97% feldspar. Therefore, most of the Sr and the REE, which leave the catchment basin by the streamwater, originate from corrosion and dissolution of feldspar and phosphate minerals. The Sr and Nd isotopic ratios further suggest that an important part of the Sr and Nd in the waters originate from leached or dissolved phosphate minerals like apatite.

Acknowledgments—We thank G. Bracke, F. Chabaux, and F. Gauthier-Lafaye for fruitful discussions. The technical assistance of B. Kiefel, J. Samuel, R. Rouault, G. Krempp, Y. Hartmeier, and D. Million of the Centre de Géochimie de la Surface at Strasbourg is acknowledged. The constructive reviews by J. Gaillardet, S. L. Goldstein and an anonymous reviewer are gratefully acknowledged. D. A. profited from an MRT grant. This work was supported by the Region Alsace within the framework of the IFARE (Institut Franco-Allemand de Recherche pour l'Environnement).

Associate editor: S. M. McLennan

REFERENCES

Allègre C. J., Dupré B., Négrel P., and Gaillardet J. (1996) Sr-Nd-Pb isotope systematics in Amazon and Congo River systems: Constraints about erosion processes. *Chem. Geol.* **131,** 93–112.

Amiotte-Suchet P. and Probst J. L. (1995) A global model for present day atmospheric/soil CO_2 consumption by chemical erosion of continental rocks (GEM-CO_2). *Tellus* **47B,** 1/2 273–280.

Baize D. (1988) Guide des analyses courantes en pédologie. *INRA* 172 p.

Banfield J. P. and Eggleton R. A. (1989) Apatite replacement and rare earth mobilization, fractionation, and fixation during weathering. *Clays Clay Miner.* **37,** 113–127.

Banks D., Hall G., Reimann C., and Siewers U. (1999) Distribution of rare earth elements in crystalline bedrock groundwaters Oslo and Bergen regions, Norway. *Appl. Geochem.* **14,** 27–39.

Biron P., Najjar G., Viville D., Granier A., and Dambrine E. (1997) Sap flow and micrometeorological measurements in the Strengbach catchment (Vosges mountains) for SVAT model validation. In *Technical Documents in Hydrology, UNESCO* (eds. Viville and Littlewood), Proceedings of Ecohydrological Processes in Small Basins, 13–20.

Blum J. D. and Erel Y. (1997) Rb-Sr isotope systematics of a granitic soil chronosequence: The importance of biotite weathering. *Geochim. Cosmochim. Acta* **61,** 3193–3204.

Blum J. D., Erel Y., and Brown K. (1994) $^{87}Sr/^{86}Sr$ ratios of Sierra Nevada stream waters: Implications for relative mineral weathering rates. *Geochim. Cosmochim. Acta* **58,** 5019–5025.

Bonhomme M. (1967) Ages radiométriques de quelques granites des Vosges moyennes. *Bull. Carte Géol. Als. Lorr.* **20,** 101–106.

Boulange B. and Colin F. (1994) Rare earth element mobility during conversion of nepheline syenite into lateritic bauxite at Passo-Quatro, Minas Gerais, Brazil. *Appl. Geochem.* **96,** 701–711.

Braun J. J., Pagel M., Muller J. P., Bilong P., Michard A., and Guillet B. (1990) Ce anomalies in lateritic profiles. *Geochim. Cosmochim. Acta* **54,** 781–795.

Braun J. J., Pagel M., Herbillon A., and Rosin C. (1993) Mobilization and redistribution of REEs and thorium in a syenitic lateritic profile: A mass balance study. *Geochim. Cosmochim. Acta* **57,** 4419–4434.

Braun J. J., Viers J., Dupré B., Polvé M., Ndam J., and Muller J. P. (1998) Solid/liquid REE fractionation in the lateritic system of Goyoum, East Cameroon: The implication for the present dynamics of the soil covers of the humid tropical regions. *Geochim. Cosmochim. Acta* **62,** 273–299.

Brookins D. G. (1989) Aqueous geochemistry of rare earth elements. In *Reviews in Mineralogy: Geochemistry and Mineralogy of Rare Earth Elements* (eds. B. R. Lippin and G. A. McKay), **21,** 201–223.

Cantrell K. J. and Byrne R. H. (1987) Rare earth element complexation by carbonate and oxalate ions. *Geochim. Cosmochim. Acta* **51,** 597–605.

Condie K. C. (1991) Another look at rare earth elements in shales. *Geochim. Cosmochim. Acta* **55,** 2527–2531.

Condie K. C., Dengate J., and Cullers R. L. (1995) Behavior of rare earth elements in a paleoweathering profile on granodiorite in the Front Range, Colorado, USA. *Geochim. Cosmochim. Acta* **59,** 279–294.

Dambrine E., Ranger J., Nys C., Bonneau M. (1995) Cycling and budgets of acidity and nutrients in Norway spruce stands in northeastern France and the Erzgebirge (Czech Republic). In *Forest Decline and Atmospheric Deposition Effect in the French Mountains.* (eds. G. Landmann and M. Bonneau), Part 3, pp. 233–258.

Dambrine E., Pollier B., Poszwa A., Ranger J., Probst A., Viville D., Biron P., and Granier A. (1998) Evidence of current soil acidification in spruce (Strengbach catchment, Vosges mountains, North-Eastern France). *Water Air Soil Poll.* **105,** 43–52.

Douglas G. B., Gray C. M., Hart B. T., and Beckett R. (1995) A strontium isotopic investigation of the origin of suspended particulate matter (SPM) in the Murray-Darling River system, Australia. *Geochim. Cosmochim. Acta* **59,** 3799–3815.

Drever J. I. and Clow D. W. (1995) Weathering rates in catchments. In *Reviews in Mineralogy. Chemical Weathering Rates of Silicate Minerals* (eds. A. F. White and S. L. Brantley), **31,** 463–483.

Dupré B., Gaillardet J., Rousseau D., and Allègre C. J. (1996) Major and trace elements of river-borne material: The Congo basin. *Geochim. Cosmochim. Acta* **60,** 1301–1321.

Elderfield H., Upstill-Goddard R., and Sholkovitz E. R. (1990) The rare earth elements in rivers, estuaries, and coastal seas and their significance to the composition of ocean waters. *Geochim. Cosmochim. Acta* **54,** 971–991.

El Gh'Mari A. (1995) Etude minéralogique, pétrophysique et géochimique de la dynamique d'altération d'un granite soumis au dépĉts atmosphériques acides (Bassin versant du Strengbach, Vosges, France) mécanismes, bilans et modélisations. Ph.D. thesis, ULP Strasbourg, 202 p.

Fichter J. (1997) Minéralogie quantitative et flux d'éléments minéraux libéré par altération des minéraux des sols dans deux écosystèmes sur granite (Bassin versant du Strengbach, Vosges). Ph.D thesis, Univ. Henri Poincaré Nancy, 284 p.

Fichter J., Turpault M. P., Dambrine E., and Ranger J. (1998) Mineral evolution of acid forest soils in the Strengbach catchment (Vosges Mountains, N-E France). *Geoderma.* **82,** 315–340.

Gaillardet J., Dupré B., and Allègre C. J. (1995) A global geochemical mass budget applied to the Congo Basin rivers: Erosion rates and continental crust composition. *Geochim. Cosmochim. Acta* **59,** 3469–3485.

Gaillardet J., Dupré B., Allègre C. J., and Négrel P. (1997) Chemical

and physical denudation in the Amazon river basin. *Chem. Geol.* **142,** 141–173.
Goldstein S. J. and Jacobsen S. B. (1987) The Nd and Sr isotopic systematics of river-water dissolved material: Implications for the sources of Nd and Sr in seawater. *Chem. Geol.* **66,** 245–272.
Goldstein S. J. and Jacobsen S. B. (1988a) Rare earth elements in river waters. *Earth Planet. Sci. Lett.* **89,** 35–47.
Goldstein S. L. and Jacobsen S. B. (1988b) Nd and Sr isotopic systematics of river water suspended material: Implications for crustal evolution. *Earth. Planet. Sci. Lett.* **87,** 249–265.
Goldstein S. L., O'Nions R. K., and Hamilton P. J. (1984) A Sm-Nd isotopic study of atmospheric dusts and particulates from major river systems. *Earth Planet. Sci. Lett.* **70,** 221–236.
Graustein W. C. and Armstrong R. L. (1983) The use of strontium-87/strontium-86 ratios measure atmospheric transport into forested watersheds. *Science* **219,** 289–292.
Henry F., Probst J. L., Thouron D., Depetris P., and Garçon V. (1996) Nd-Sr isotopic compositions of dissolved and particulate material transported by the Parana and Uruguay rivers during high and low water periods. *Sci. Géol. Bull.* **49,** 1–3.
Idir S., Probst A., Viville D., and Probst J. L. (1999) Contribution des surfaces saturées et des versants aux flux d'eau et d'éléments exportés en période de crue: Traçage à l'aide du carbone organique dissous et de la silice. Cas du petit bassin versant du Strengbach (Vosges, France). *C.R. Acad. Sci.* **328,** 101–106.
Ingri J., Widerlund A., Land M., Gustafsson Ö., Andersson P., and Öhlander, B. (2000). Temporal variations in the fractionation of the rare earth elements in a boreal river; the role of colloidal particles. *Chem. Geol.* **166,** 23–45.
Johannesson K. H., Stetzenbach K. J., Hodge V. F., and Lyons W.B. (1996) Rare earth element complexation behavior in circumneutral pH groundwaters: Assessing the role of carbonate and phosphate ions. *Earth Planet. Sci. Lett.* **139,** 305–319.
Koppi A. J., Edis R., Field D. J., Geering H. R., Klessa D. A., and Cockayne D. J. H. (1996) Rare earth element trends and cerium-uranium-manganese associations in weathered rock from Koongarra, Northern Territory, Australia. *Geochim. Cosmochim. Acta* **60,** 1695–1707.
Ladouche B., Probst A., Viville D., Idir S., Baqué D., Loubet M., Probst J. L., and Bariac T. (in press). Hydrograph separation using isotopic, chemical and hydrological approaches (Strengbach catchment, France). *J. Hydrology*.
Langmuir D. and Herman J. S. (1980) The mobility of thorium in natural waters at low temperatures. *Geochim. Cosmochim. Acta* **44,** 1753–1766.
Lu P., Biron P., Breda N., and Granier A. (1995) Water relations of adult Norway spruce (Picea abies (L) Karst) under soil drought in the Vosges mountains: Water potential, stomatal conductance and transpiration. *Ann. Sci. For.* **52,** 117–129.
Martin J. M. and Meybeck M. (1979) Element mass-balance of material carried by major world rivers. *Mar. Chem.* **7,** 173–206.
McLennan S.M. (1989) Rare earth elements in sedimentary rocks: Influence of provenance and sedimentary processes. In: *Reviews in Mineralogy. Geochemistry and Mineralogy of Rare Earth Elements* (eds. B. R. Lippin and G. A. McKay), **21,** 169–200.
Meybeck M. (1987) Global chemical weathering from surficial rocks estimated from river dissolved loads. *Am. J. Sci.* **287,** 401–428.
Miller E. K., Blum J. D., and Friedland A. J. (1993) Determination of soil exchangeable-cation loss and weathering rates using Sr isotopes. *Nature* **362,** 438–441.
Minarik L., Zigova A., Bendl J., Sktivan P., and Stastny M. (1998) The behaviour of rare-earth elements and Y during the rock weathering and soil formation in the Ricany granite massif, Central Bohemia. *Sci. Total Environ.* **215,** 101–111.
Munier-Lamy C. (1987) Mobilisation et préconcentration de l'uranium dans les sols: Rôle des substances humiques. Ph.D thesis, Univ. Nancy I, Nancy, 208 p.
Négrel P., Allègre C. J., Dupré B., and Lewin E. (1993) Erosion sources determined by inversion of major and trace element ratios in river water: The Congo basin case. *Earth Planet. Sci. Lett.* **120,** 59–76.
Nesbitt H. W. (1979) Mobility and fractionation of rare earth elements during weathering of a granodiorite. *Nature* **279,** 206–210.
Nesbitt H. W. and Markovics G. (1997) Weathering of granodiorite crust, long-term storage of elements in weathering profiles, and petrogenesis of siliclastic sediments. *Geochim. Cosmochim. Acta* **61,** 1653–1670.
Nesbitt H. W., MacRae N. D., and Kronberg B. J. (1990) Amazon deep-sea fan muds: Light REE enriched products of extreme chemical weathering. *Earth Planet. Sci. Lett.* **100,** 118–123.
Pfister L., Viville D., Najjar G., Biron P., Richard S., and Fischer L. (1997) A new concept for canopy water storage simulation in a 30-years old spruce stand (Strengbach catchment, Vosges, France). In *Technical Documents in Hydrology, UNESCO* (eds. Viville and Littlewood), Proceedings of Ecohydrological Processes in Small Basins, 7–12.
Probst A., Dambrine E., Viville D., and Fritz B. (1990) Influence of acid atmospheric inputs on surface water chemistry and mineral fluxes in a declining spruce stand within a small granitic catchment (Vosges massif, France). *J. Hydrol.* **116,** 101–124.
Probst A., Viville D., Fritz B., Ambroise B., and Dambrine E. (1992) Hydrochemical budgets of a small forested granitic catchment exposed to acid deposition: The Strengbach catchment case study (Vosges Massif, France). *Water Air Soil Poll.* **62,** 337–347.
Probst A., Fritz B., and Viville D. (1995a) Mid-term trends in acid precipitation, streamwater chemistry and element budgets in the Strengbach catchment (Vosges Mountains, France). *Water Air Soil Poll.* **79,** 39–59.
Probst A., Lelong F., Viville D., Durand P., Ambroise B., and Fritz B. (1995b) Comparative hydrochemical behavior and elements budgets of the Aubure (Vosges Massif) and Mont Lozère (Massif Central) spruce forested catchments. In Forest Decline and Atmospheric Deposition Effect in the French Mountains (eds. G. Landmann and M. Bonneau), Part. 3, pp. 203–225. Springer, Berlin.
Probst A., El Gh'Mari A., Aubert D., Fritz B., and McNutt R. (2000). Strontium as a tracer of weathering processes in a silicate catchment polluted by acid atmospheric inputs, Strengbach, France. *Chem. Geol.* (in press).
Riotte J. and Chabaux F. (1999) ($^{243}U/^{238}U$) activity ratios in freshwaters as tracers of hydrological processes: The Strengbach watershed, Vosges, France. *Geochim. Cosmochim. Acta* **63,** 1263–1275.
Santchi P. H. and Honeyman B. D. (1991) Radioisotopes as tracers for the interactions between trace elements, colloids and particles in natural waters. In *Heavy Metals in the Environment* (ed. J. P. Vernet), pp. 229–246. Elsevier, Amsterdam,
Shabani M. B., Agaki T., and Masuda A. (1992) Preconcentration of trace rare earth elements in seawater by complexation with HDEHP and H2MEHP adsorbed on a C18 cartridge and determination by inductively coupled plasma mass spectrometry. *Anal. Chem.* **64,** 737–743.
Sharma A. and Rajamani V. (2000). Weathering of gneissic rocks in the upper reaches of Cauvery river, south India: Implications to neotectonics of the region. *Chem. Geol.* **166,** 203–223.
Sholkovitz, E. R. (1989) Artifacts associated with the chemical leaching of sediments for rare earth elements. *Chem. Geol.* **77,** 47–51.
Sholkovitz E. R. (1992) Chemical evolution of rare earth elements: Fractionation between colloidal and solution phases of filtered river water. *Earth Planet. Sci. Lett.* **114,** 77–84.
Sholkovitz E. R., Landing W. M., and Lewis B. L. (1994) Ocean particle chemistry: The fractionation of rare earth elements between suspended particles and seawater. *Geochim. Cosmochim. Acta* **58,** 1567–1579.
Stallard R. F. and Edmond J. M. (1983) Geochemistry of the Amazon 2. The influence of geology and weathering environment on the dissolved load. *J. Geophys. Res.* **88,** 9671–9688.
Steinmann M. and Stille P. (1997) Rare earth element behavior and Pb, Sr, Nd isotope systematics in a heavy metal contaminated soil. *Appl. Geochem.* **12,** 607–624.
Stille P. and Clauer N. (1994) The process of glauconitization: Chemical and isotopic evidence. *Contrib. Mineral. Petrol.* **117,** 253–262.
Stille P., Gauthier-Lafaye F., and Louvat D. (1999) REE migration in groundwaters close to the natural fission reactor of Bangombé (Gabon); Sm-Nd isotope evidence. In Proceedings of the Oklo Phase II Workshop (eds. D. Louvat, V. Michaud and H.v. Maravic). EUR Report Series nº 19137, pp. 263–272, Brussels.

Stordal M. C. and Wasserburg G. J. (1986) Neodymium isotopic study of Baffin Bay water: Sources of REE from very old terranes. *Earth Planet. Sci. Lett.* **77,** 259–272.

Tricca A. (1997) Transport mechanism of trace elements in surface and ground water: Sr, Nd, U isotope and REE evidence. Unpubl. Ph.D. thesis, Université Louis Pasteur de Strasbourg.

Tricca A., Stille P., Steinmann M., Kiefel B., Samuel J., and Eikenberg J. (1999) Rare earth elements and Sr and Nd isotopic compositions of dissolved and suspended loads from small river systems in the Vosges mountains (France), the river Rhine and the groundwater. *Chem. Geol.* **160,** 139–158.

Viers J., Dupré B., Polvé M., Schott J., Dandurand J. L., and Braun J. J. (1997) Chemical weathering in the drainage basin of a tropical watershed (Nsimi-Zoetele site, Cameroon): Comparison between organic-poor and organic-rich waters. *Chem. Geol.* **140,** 181–206.

Viville D., Biron P., Granier A., Dambrine E., and Probst A. (1993) Interception in a mountainous declining spruce stand in the Strengbach catchment (Vosges, France). *J. Hydrol.* **144,** 273–282.